



A11105 983570

REFERENCE

NBS  
Publi-  
cations**NBSIR 84-2874R**

# **CSIR: A Two-Dimensional Finite Element Charge-Sheet Model of MOSFET's Including Radiation-Induced Interface and Oxide Charge**

---

U.S. DEPARTMENT OF COMMERCE  
National Bureau of Standards  
National Engineering Laboratory  
Center for Electronics and Electrical Engineering  
Semiconductor Devices and Circuits Division  
Washington, DC 20234

May 1984

Prepared for  
**Defense Nuclear Agency**  
**Washington, DC**

QC  
100  
U56  
84-2874R  
1984



Ref  
QC  
160  
456  
84-2874R  
1984

NBSIR 84-2874R

**CSIR: A TWO-DIMENSIONAL FINITE  
ELEMENT CHARGE-SHEET MODEL OF  
MOSFET'S INCLUDING RADIATION-INDUCED  
INTERFACE AND OXIDE CHARGE**

---

C. L. Wilson and J. L. Blue

U.S. DEPARTMENT OF COMMERCE  
National Bureau of Standards  
National Engineering Laboratory  
Center for Electronics and Electrical Engineering  
Semiconductor Devices and Circuits Division  
Washington, DC 20234

May 1984

Prepared for  
Defense Nuclear Agency  
Washington, DC



---

U.S. DEPARTMENT OF COMMERCE, Malcolm Baldrige, *Secretary*  
NATIONAL BUREAU OF STANDARDS, Ernest Ambler, *Director*





## List of Figures

1. Geometry of the charge-sheet model . . . . .	4
2. A subthreshold region simulation compared to measured data for an unirradiated transistor . . . . .	15
3. A subthreshold region simulation compared to measured data for a 10 Krad(Si) dose . . . . .	16
4. A subthreshold region simulation compared to measured data for a 50 Krad(Si) dose . . . . .	17
5. A subthreshold region simulation compared to measured data for a 100 Krad(Si) dose . . . . .	18
6. A subthreshold region simulation compared to measured data for a 500 Krad(Si) dose . . . . .	19
7. A subthreshold region simulation compared to measured data for a 500 Krad(Si) dose, trap distribution peaked near the valence band . . . . .	20
8. A saturation region simulation compared to measured data for an unirradiated transistor . . . . .	21
9. A saturation region simulation compared to measured data for a 500 Krad(Si) dose . . . . .	22
10. The triode region characteristics, as a function of dose, compared to measured data . . . . .	23

# CS1R: A Two-Dimensional Finite Element Charge-Sheet Model of MOSFETs Including Radiation-Induced Interface and Oxide Charge

C. L. Wilson<sup>†</sup> and J. L. Blue  
National Bureau of Standards  
Washington, DC 20234

## Abstract

A two-dimensional charge-sheet model including radiation-induced interface and oxide effects in short-channel MOS transistors has been developed. The unique feature of the model is that the effects of channel inversion layer charge, interface charge, and oxide charge are included as a nonlinear integral boundary condition on the two-dimensional electrostatic field in the transistor. The average inversion layer charge density and source-drain current are obtained directly from the model rather than from the electron density or electron quasi-Fermi level. The model retains all of the physical detail of more complex two-dimensional models such as sensitivity to source-drain profile shape, channel profile, and oxide field shape. This allows the model to represent the changes in drain current associated with short-channel effects while still allowing simple comparison with long-channel models.

The numerical solutions were obtained using general-purpose software for solving elliptic partial differential equations. Problems with exact solutions have been solved to test the correctness and accuracy of the codes. Also, the physics included in this model and the geometry of the transistor can be easily changed. The finite element method used allows refinement of oblique triangles which is important in achieving computational efficiency.

Key words: finite elements; interactive graphics; MOS transistors; radiation effects.

## 1. Introduction

A two-dimensional formulation of a charge-sheet model of an MOS transistor and an associated computer program are presented. This formulation differs from the formulation of De La Moneda [1] in that it includes the effects of source-drain channel shape and arbitrary channel doping profile shape. The formulation differs from the formulation proposed by Brews [2] in that strong two-dimensional electro-

<sup>†</sup> The work of the first author sponsored by the Defense Nuclear Agency under Task X99QAXVX, Work Unit 00076.

static effects are included by solving Poisson's equation using adaptive finite element techniques in the bulk semiconductor. In this formulation, a new approach that differs from both [1] and [2] is used to couple the one-dimensional current to the two-dimensional potential. The effects of the charge in the inverted channel of the transistor are included as a nonlinear boundary condition at the interface between the semiconductor and the gate oxide.

The principal modification of the program, from the original CS1 [3,4] program, is accomplished by modifying the surface boundary condition. The primary effect of ionizing radiation on MOSFETs is the introduction of oxide trapped charge (OTC), interface trapped charge (ITC), and the reduction of channel mobility caused by scattering from charge in interface traps. Both of the charge effects must be included in the oxide interface boundary condition. The OTC is independent of device operating voltage after irradiation, while the charge state of the ITC is dependent on gate bias in the subthreshold and weak inversion regions since the probability of these traps being occupied is a function of the local surface potential in the two-dimensional model. Inclusion of these two charge components in device models introduces a nonscalable component into the calculation of the total effective channel charge in short-channel transistors.

The charge-sheet formulation allows the two-dimensional electrostatic field and drain current to be calculated without the inclusion of a two-dimensional current continuity equation. This results in a great improvement in computational efficiency which allows finite element model calculations to be performed on a minicomputer. This model is accurate in all regions of inverted transistor operation and works well even in regions of operation where the channel current produces large changes in the electrostatic potential in the channel. The model retains the computational efficiency of single equation models [5] without imposing the computer requirements of coupled equation models [6,7,8]. The complexity and cost of the model lie between the long-channel one-dimensional model of Brews, which runs well on a desk top calculator, and the coupled equation models, which are best suited to large computers. Unlike previous single equation models [5], the two-dimensional charge-sheet model works in all regions of inverted transistor operation including weak inversion. Use of the finite-element method also allows the adaptive mesh procedures [9] previously applied to MESFETs [10] to be applied to MOSFETs.

In section two, the formulation of the two-dimensional charge-sheet model and the effect of ITC and OTC at the semiconductor-oxide interface are discussed. In this formulation, the total channel current is computed as a function of the two-dimensional electrostatic potential. The computation of total channel current allows the effects of these mobile and fixed charges to be treated as an effective surface



charge and to be included in subsequent calculations of the electrostatic potential as a nonlinear integral boundary condition.

In section two, the numerical procedures used to calculate the electrostatic potential in two dimensions with a nonlinear boundary condition are also discussed. The partial differential equation is transformed into a system of nonlinear equations using adaptive, computer-generated, finite elements. The nonlinear field equations are solved using a damped Newton's method. The resultant system of linear equations is solved either by direct methods or by a multilevel iteration.

In section three, the specific procedures used to implement the model are discussed. The structure of the computer program is discussed and the function of each of the principal modules is outlined. The installation requirements of the program are discussed as are the sources of the software components which were developed by other authors. The physical limitations of the model are then discussed.

In section four, the modeling of a set of irradiated MOS transistors is discussed.

## 2. Theory

### A. Two-Dimensional Charge-Sheet Model

The two-dimensional charge-sheet model used in this work couples the effects of the interface trapped charge and the oxide trapped charge to short-channel effects seen in unscaled MOSFETs. In this work, a two-dimensional finite element model of short-channel MOSFETs is applied which allows the effects of ITC and OTC, as well as radiation-induced channel mobility degradation, to be included in a two-dimensional short-channel MOSFET model. The basic formulation of the model includes a two-dimensional calculation of the electrostatic potential in the channel region and in the oxide and a one-dimensional calculation of the channel inversion layer current. This simplification is achieved by making assumptions based on the basic semiconductor equations:

$$\nabla \cdot (\kappa \nabla \psi) = -\frac{q}{\epsilon_0}(p - n + N) \quad (1)$$

$$\nabla \cdot (\mu_n n \nabla \phi_n) = \frac{\partial n}{\partial t} + R \quad (2)$$

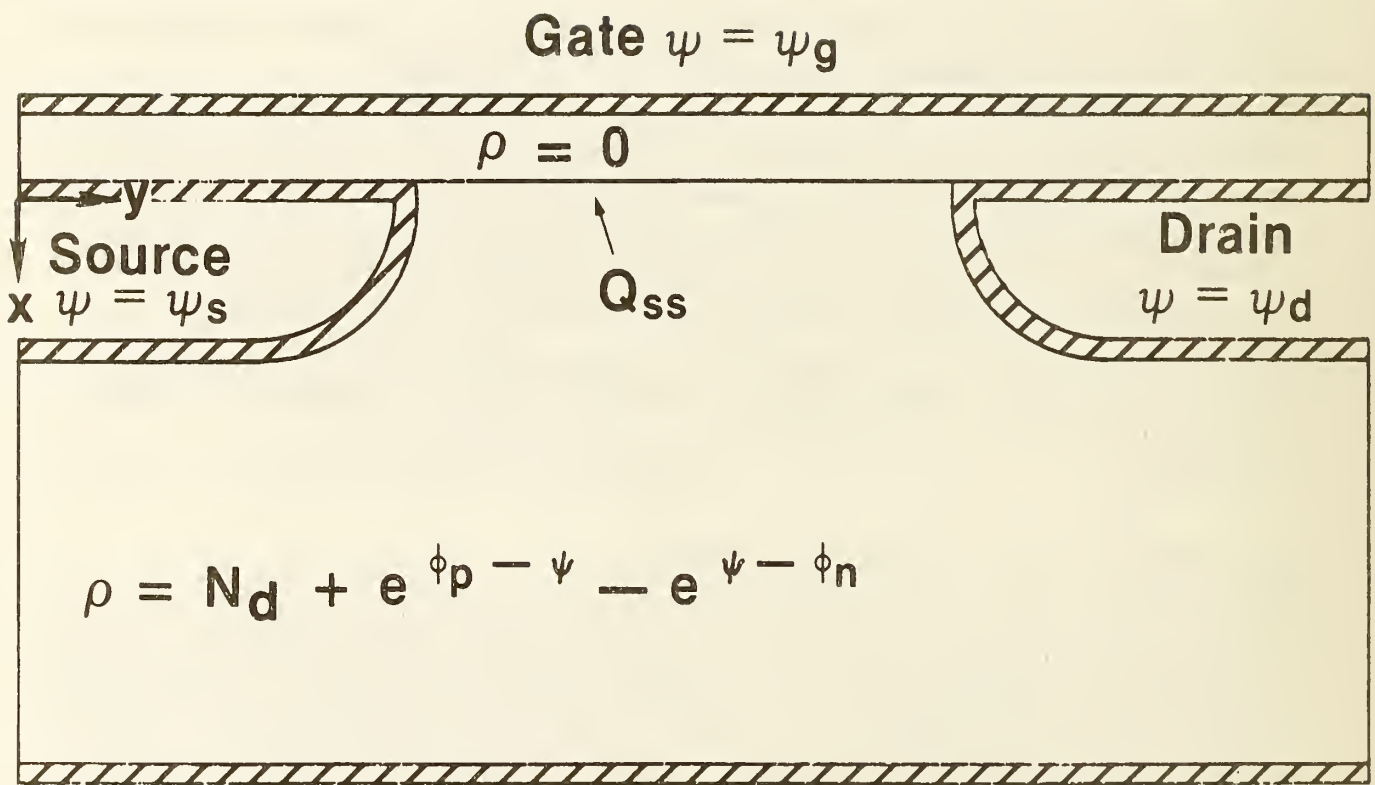


Figure 1. Geometry of the charge-sheet model.

$$\nabla \cdot (\mu_p p \nabla \phi_p) = \frac{\partial p}{\partial t} - R, \quad (3)$$

where the electron density,  $n$ , and the hole density,  $p$ , are:

$$n = n_i \exp(q(\psi - \phi_n)/kT) \quad (4)$$

$$p = n_i \exp(q(\phi_p - \psi)/kT), \quad (5)$$

and where Shockley-Read-Hall recombination is given by:

$$R = \frac{(pn - n_i^2)}{\tau_{n0}(n + n_1) + \tau_{p0}(p + p_1)}. \quad (6)$$

The symbols have their usual meaning as defined in [12].

The simplification to a single two-dimensional equation and one-dimensional current flow is achieved by assuming that  $R = 0$ , which eliminates (6), and that the hole quasi-Fermi potential is pinned at the substrate potential,  $\phi_p = V_{sub}$ . This is then used to replace (5) and eliminate (3). If in addition the channel current is assumed to flow only in a one-dimensional sheet at the surface, the problem is reduced to solving (1) and:

$$n(y) = \frac{n_i}{\mu_n^*} \int_0^\infty dx \exp(\beta\psi)\mu_n \left[ 1 + (\exp(-\beta V_D) - 1) \frac{\int_0^y \frac{dy_0}{\int_0^\infty dx \exp(\beta\psi)\mu_n}}{\int_0^L \frac{dy_0}{\int_0^\infty dx \exp(\beta\psi)\mu_n}} \right]. \quad (7)$$

Equation (7) then replaces (2). The effects of OTC and ITC are included in the oxide solution and in the interface boundary condition connecting the oxide field solution to the solution in the bulk semiconductor. One of the advantages of the finite element formulation of the model is that the interfacial charge can be treated exactly in the calculation of the finite element equations and in oxide boundary conditions. If in addition the depletion in the source and drain regions is neglected, the problem is reduced to the geometry shown in figure 1.

In this formulation of the problem, the OTC and ITC are given by:

$$Q_{itc} = f(Dose) \quad (8)$$

$$Q_{otc} = g(Dose)\nabla\psi_{ox} \quad (9)$$

where:

$$Q_{itc}(\phi_S) = \int_{E_v}^{E_c} \frac{Q(E_d)dE_d}{1 + g_d \exp((\phi_S - E_d)/kT)} - \int_{E_v}^{E_c} \frac{Q(E_a)dE_a}{1 + g_a^{-1} \exp((E_a - \phi_S)/kT)} \quad (10)$$

$$Q_{itc}(\phi_S) \approx \sum_{\Delta E} \frac{Q(E_d)\Delta E_d}{1 + g_d \exp((\phi_S - E_d)/kT)} - \sum_{\Delta E} \frac{Q(E_a)\Delta E_a}{1 + g_a^{-1} \exp((E_a - \phi_S)/kT)} \quad (11)$$

The specific relationships between dose and these charge components in (8) and (9) are very technology specific and must be determined by the program user.

## B. Numerical Procedures

An important feature of this work is that the numerical solutions were obtained using general-purpose software for solving elliptic partial differential equations (PDEs). Although some efficiency is sacrificed, the benefits obtained by using the general-purpose software far outweigh the loss in efficiency. Problems with exact solutions have been solved to test the correctness and accuracy of the codes and to determine optimal strategies and optimal values for parameters in the code. The physics included in the model and the geometry of the problem can be easily changed. The numerical software was inspired by finite-element software of Bank and Sherman [9] and retains most of their philosophy.

This version of the package solves the PDE

$$\nabla \cdot [a(x, y, u)\nabla u] = f(x, y, u, \partial u/\partial x, \partial u/\partial y) \quad (12)$$

in a region bounded by straight line segments and circular arc segments. On each segment of the boundary,  $u$  must obey one of two types of boundary conditions (1):

$$g(x, y, u) = 0 \quad (13)$$

or (2)

$$\partial u / \partial \mathbf{n} + g(x, y, u) = 0. \quad (14)$$

This is a fairly general example of a PDE arising from conservation of a flux and includes both Poisson's equation and the hole and electron continuity equations (in the multiple-PDE version).

At the heart of the package is a module which solves a linear elliptic PDE using linear finite elements on a mesh of triangles. (Boundary "triangles" may have one curved side.) The initial triangulation is an input to the package; succeeding triangulations are calculated adaptively by the package.

For a given triangulation with  $M$  vertices, the calculation proceeds as follows.

The  $M$  finite-element basis functions  $\{b_m\}$  are linear on each triangle;  $b_m$  is 1 at vertex  $m$  and 0 at all other vertices. The set of vertices on type 1 boundaries is denoted by  $D$  (for Dirichlet). The solution is approximated by a sum of basis functions

$$u(x, y) = \sum_{m=1}^M \alpha_m b_m(x, y). \quad (15)$$

The coefficients are determined by a Galerkin method [13]; the error in the PDE is made orthogonal to each of the basis functions except those in  $D$ :

$$\int \int [(-\nabla \cdot (a \nabla u) + f) b_m]_{\substack{m=1,2,\dots,M \\ m \text{ not in } D}} = 0. \quad (16)$$

The remaining conditions on the  $b$ 's are that the type 1 boundary conditions hold exactly [13]:

$$g(x_m, y_m, u(x_m, y_m)) = 0, m \text{ in } D. \quad (17)$$

Equation (16) is integrated by parts to yield

$$\int \int (a \nabla u \cdot \nabla b_m + f b_m) + \int_2 a g b_m = 0, \quad (18)$$

where the single integral is over the type-2 parts of the boundary only. Equations (17) and (18) comprise  $M$  nonlinear equations in  $M$  unknowns, the coefficients  $\{\alpha_m\}$ .

The  $M$  nonlinear equations are solved by an iterative process, a damped Newton's method. Let  $v$  be the Newton step and use a fraction of  $v$  as a correction to  $u$ ;  $v$  has the same form as  $u$ ,

$$v(x, y) = \sum_{m=1}^M \beta_m b_m(x, y). \quad (19)$$

To calculate  $v$ , replace  $u$  by  $u + v$  in eqs (17) and (18) and linearize in  $v$ . The linearization of eq (17) yields

$$g(x_m, y_m, u_m) + \frac{\partial g(x_m, y_m, u_m)}{\partial u} \beta_m = 0, m \text{ in } D, \quad (20)$$

and the linearization of eq (18) yields

$$\left\{ a \nabla v \cdot \nabla b_m + \frac{\partial a}{\partial u} v \nabla u \cdot \nabla b_m + b_m \left( \frac{\partial f}{\partial u} v + \frac{\partial f}{\partial(\partial u / \partial x)} \frac{\partial v}{\partial x} + \frac{\partial f}{\partial(\partial u / \partial y)} \frac{\partial v}{\partial y} \right) \right\} + \int_2 \left( g \frac{\partial a}{\partial u} + a \frac{\partial g}{\partial u} \right) b_m = - \int \int (a \nabla u \cdot \nabla b_m + f b_m) - \int_2 a g b_m \equiv r_m \quad (21)$$

Substituting for  $u$  and  $v$  from eqs (15) and (19) and doing the integrals numerically gives a set of  $M$  linear equations for the correction coefficients  $\{\beta_m\}$ . These linear equations are sparse; there are typically only nine nonzero elements per row, on average, and  $M$  can be a few hundred or a few thousand. A satisfactory way to solve these equations is directly, with Gaussian Elimination, using the Yale Sparse Matrix Package [14].

Unless  $u$  is close to a solution of the nonlinear finite-element equations,  $u + v$  may be worse than  $u$ . A damped Newton's method is used: replace  $u$  by  $u + \lambda v$ , where  $\lambda$  is chosen so that  $\max_m |r_m(u + v)| < \max_m |r_m(u)|$ . This avoids divergence of the iterative process.

In practice, the initial triangulation may be too coarse to give the desired accuracy or may need local refinement to represent the solution accurately in a region of high curvature. After the package has converged to an approximate solution on the initial triangulation, the approximate solution may be used to estimate the error and produce a new and finer triangulation adaptively. There are various ways to approximate the error in each triangle. For the present work, a simple method is used. In the silicon, the PDE is

$$\nabla^2 \psi = -\rho/\epsilon. \quad (22)$$

Since  $\psi$  is linear in each triangle,  $\nabla^2 \psi = 0$ . We estimate the relative error in each triangle by

$$\left| \int_{\text{triangle}} \int \rho(x, y) \right|. \quad (23)$$

The refined triangulation is obtained by dividing the triangles with the largest

estimated errors, such as all triangles with estimated error larger than 1/4 of the largest error.

For the refined triangulation, the previously calculated  $u$  is a good guess at the new  $u$ , so that few Newton iterations should be necessary. The hardest work is done on the initial triangulation, the one with the fewest vertices.

If there are two or more triangulations, the linear equations on the finest triangulation may be solved by a multilevel iteration [15,9], saving both time and storage space. However, for the present problem, sufficient accuracy could be obtained with  $M$  of only a few hundred, so that a direct solution using the Yale Sparse Matrix Package was quite adequate.

Using this procedure, the solution of eqs (1) and (7) is started by first obtaining a trial solution for the linearized form of eq (1), using the solution of eq (7) obtained from the one-dimensional charge-sheet model with the total charge as a boundary condition. The Jacobian of  $g$  required for the solution of eq (20) contains the Jacobian of eq (1). This Jacobian is approximated by

$$\frac{\partial g}{\partial u} = q\beta(n(y) + Q_{itc} + Q_{otc}). \quad (24)$$

Once the surface charge and approximate local field term are obtained from the one-dimensional model and a local-field condition, the field term associated with the oxide is obtained using a fast Poisson solver [16]. The trial solution is then used to obtain a solution for eq (7) by quadrature and an additional fast Poisson solution in the oxide. This iterative procedure is repeated for each Newton step until the requested convergence is obtained or the specified maximum iteration count is reached.

### 3. Computer Implementation

#### A. Software Modules

The distributed source of the CS1R program is divided into four files: CS1R.FOR, SYSTEM.FOR, PDESUB.FOR, and DEVLIB.FOR. These four files conform to ANSI 66 FORTRAN IV and can be compiled on any FORTRAN compiler which meets this standard. The files CS1R.HLP, CS1R.EXP, and CS1R.LNK are also provided. CS1R.HLP provides a set of user instructions identical to Appendix A of this report. CS1R.EXP contains an example set of program input and output



which is identical to Appendix B of this report. The file CS1R.LNK is a sample set of linkage control statements which have been used to link the program on the DEC VAX 11/780\* under the VMS\* system.

The file CS1R.FOR is the actual charge-sheet model program. This file contains the subroutines which control input and output, model initial approximations, find the oxide field solution, and contain the calls to the subroutines which solve the partial differential equation. The starting approximation is identical to the charge-sheet model originally developed by Brews [2]. The output of this long-channel model is printed at the beginning of each CS1R calculation. The oxide solution is calculated using the fast methods discussed in reference [16]; these subroutines are in the file DEVLIB.FOR. A complete copy of the Swarztrauber and Sweet package [16] is not included. Only those parts of the package that are used by CS1R are included.

The CS1R module of the program contains parameters TOL and IP(6) which are used to control the accuracy of the solution. The parameter TOL is used to control the iteration accuracy at each multigrid level. The parameter IP(6) is used to control the number of multigrid levels. These parameters are set to yield very accurate solutions in the version of the program which is distributed. This level of accuracy greatly exceeds that required for most applications, but is necessary, during installation and testing, to verify that the program has been correctly installed. Resetting these parameters to lower accuracy by increasing the iteration tolerance and/or decreasing the number of multigrid levels will greatly improve run times.

The file SYSTEM.FOR contains subroutines which are used in the other three program files but which are system dependent. The subroutines FOPEN and FCLOSE are used to open and close input and output files. In the VAX VMS version supplied on the tape, the file FCLOSE is a dummy subroutine. The subroutines ISTEIME and IFTIME are used to start and stop clocks which are used to measure the execution times of the parts of the partial differential solution process. If these routines are not used and dummy subroutines are substituted, ISTEIME must be less than, NOT equal to, IFTIME. If these subroutines are dummy routines, then the timing information in the output summary will be incorrect.

The subroutines PLTUTL, CURVEA, and ISCALE contain calls to vector graphics subroutines. The calls in the supplied program can be used with the TCS software

\* Certain commercial equipment, instruments, or materials are identified in this paper in order to adequately specify the experimental procedure. Such identification does not imply recommendation or endorsement by the National Bureau of Standards, nor does it imply that the materials or equipment identified are necessarily the best available for the purpose.

supplied by Tektronix\* and can be used to drive either Tektronix or Hewlett-Packard\* terminals. Other graphics packages can easily be substituted if the necessary initialization, absolute motion, and absolute vector drawing primitives are available in either software or terminal firmware. If these subroutines are made into dummy subroutines, graphics output will not be available from the program except through the plot output file. The data written into the plot output file, file 2, are a sequence of non-negative x- and y-coordinate pairs. The first line of the file contains the minimum and maximum values of the x- and y-coordinates. Each plot is terminated by a set (or sets) of negative coordinate pairs. The subroutines R1MACH, D1MACH, and I1MACH are used to set machine constants which are used in the other program modules to set machine-dependent quantities. The original versions of the functions are discussed in reference [17] as are the procedures used to generate these constants for a type of computer which is not presently included in the present list. The conversion of the program from one computer type to another should not require modification of any part of the program which is not in the SYSTEM.FOR module. This assumes that some plotting package is available and that timing subroutines are available on the target computer system.

The module PDESUB.FOR contains the subroutines used to solve the partial differential equations. The theory of these subroutines has been discussed in section 2B above.

The module DEVLIB.FOR contains subroutines used by the other three modules. These subroutines have been obtained from several sources. The error-handling software, memory management software, and machine-independent constant software were obtained from [17]. The fast elliptic solver was obtained from [16]. In the initial approximation, quadrature from [16] and root finding routines from [19] are used. In the PDESUB module, the Yale Sparse Matrix Package is used [14].

## B. Physical Restrictions

Two physical restrictions have been imposed in the present implementation of the CS1R program. First, the two-dimensional electric field dependence of the mobility has not been included. Second, the detailed slopes of the source-and-drain doping profiles have not been included in the model.

The first limitation is more serious. In circuit models and in some two-dimensional device simulation programs, the field dependence of the mobility is empirically included using an expression of the form  $a/(1 + bE)$  where  $a$  and  $b$  are empirically determined parameters and  $E$  is the magnitude of the electric field. Recent work by Cooper and Nelson [20] suggests that this model is not adequate to characterize

the field dependence of the mobility. On the other hand, the Cooper and Nelson data do not include several effects which are known to affect the low field value of the mobility; these are the effects of bulk doping and oxide interface charge. Since no definitive model for the two-dimensional dependence of the mobility is available, none has been included.

The details of the two-dimensional source-and-drain profiles are included in the model only as two elliptic abrupt junctions. This allows the details of the majority carrier quasi-Fermi level to be neglected and greatly simplifies the program, making the charge-sheet calculation much more efficient. On the other hand, at high source-drain-voltages, this approximation can lead to convergence problems and/or to inaccurate modeling of the potential near the drain. In addition, this model places the burden of specifying lateral and vertical junction depths on the program user. Other available two-dimensional device simulation programs, such as MINIMOS [6], attempt to include simple two-dimensional process models in the device modeling programs. These simplified models do not agree with more complex two-dimensional models [21] or with experimental measurement of two-dimensional junction shape [20]. If the user of the program wishes to use these simplified models, then the work of Kennedy and O'Brien can be used [23]. If more complicated models [21] or experimental data are available, then these can be used.

#### 4. Device Model Verification

The model is verified by comparing the results obtained with the model to n-channel MOSFETs of the type discussed in [24] for doses of 0, 10, 50, 100, and 500 Krad(Si). Prior to irradiation and after each irradiation, the current-voltage characteristics of the transistor were measured. Capacitance data were also taken on a MOS capacitor adjacent to the transistors. All devices were biased with +9 V on the gate or capacitor polysilicon electrode and the source, drain, and substrate grounded. The device used for model verification was chosen with a channel length of 7.8  $\mu\text{m}$  to allow the effects of radiation to be separated from short-channel effects. In this model, the interface traps are treated as a continuous distribution of traps which are populated and depopulated as the surface potential is varied. At doses below 50 Krad(Si), the effect of the energy distribution of the traps is small. Above 50 Krad(Si), the energy distribution becomes important. At a dose of 500 Krad(Si), the effect of energy distribution on subthreshold current is most sensitive to the trap energy distribution. Two-dimensional simulations were then carried out which used fixed oxide charge, a variable distribution of interface traps and channel mobility degradation to model the effects of the radiation.

All of the transistors studied were modeled in the subthreshold region, the triode

region, and the saturation region. The parameters used in these simulations are given in table 1.

Table 1.  
Simulation Parameters

$L_{ch}$	7.8	$\mu\text{m}$
$Q_{itc}$	0.0 to $1.75 \times 10^{12}$	$\text{cm}^{-2}$
$V_G, V_D$	0.5 V to 4.0 V, 0.25 V	
$t_{ox}$	0.0523	$\mu\text{m}$
$N_{ch}$	$1.5 \times 10^{16}$	$\text{cm}^{-3}$
$L_{jun}$	0.710	$\mu\text{m}$
$D_{jun}$	0.875	$\mu\text{m}$

Detailed comparison of the model with measured data shows excellent agreement between the model and measured current-voltage characteristics in the subthreshold region, the triode region, and the saturation region. A typical subthreshold region simulation is compared to measured data in figure 2 for an unirradiated sample. A typical subthreshold region simulation is compared to measured data in figure 3 for a 10 Krad(Si) dose. A typical subthreshold region simulation is compared to measured data in figure 4 for a 50 Krad(Si) dose. A typical subthreshold region simulation is compared to measured data in figure 5 for a 100 Krad(Si) dose.

As the dose is increased above 50 Krad(Si), the effects of the interface trapped charge energy distribution become increasingly important. This effect is illustrated in figures 6 and 7. In figure 6, the subthreshold characteristic of a device irradiated at 500 Krad(Si) is simulated with a uniform energy distribution of traps in the band. In figure 7, the subthreshold characteristic of a device irradiated at 500 Krad(Si) is simulated with an energy distribution of traps in the band that is peaked on the valence band side of the band gap. In both simulations, a total trap density of  $1.75 \times 10^{12} \text{cm}^{-2}$  was used. In the uniform case, the traps are populated continuously as the channel is inverted. In the second case, the populated trap density increases more rapidly as the transistor enters strong inversion.

A typical saturation region simulation is compared to measured data in figure 8 for an unirradiated sample. A typical saturation region simulation is compared to measured data in figure 9 for a 500 Krad(Si) dose. The triode region characteristics, as a function of dose, are compared to measured data in figure 10. In the radiation-hardened n-channel transistor modeled here, the effects of oxide charge and interface charge both increase linearly with dose. These two charges cancel to

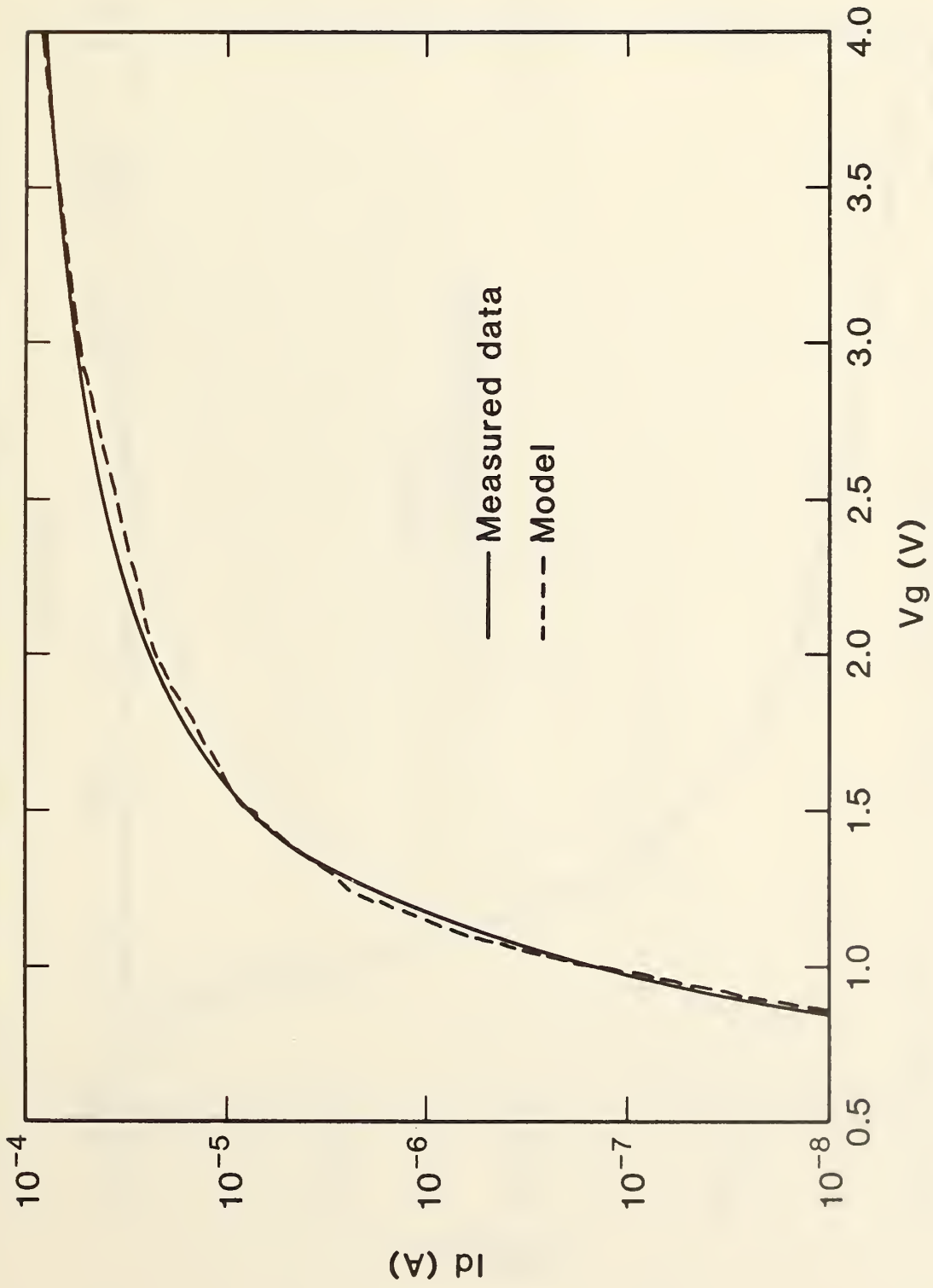


Figure 2. A subthreshold region simulation compared to measured data for an unirradiated transistor,  $V_d=0.25$  V.

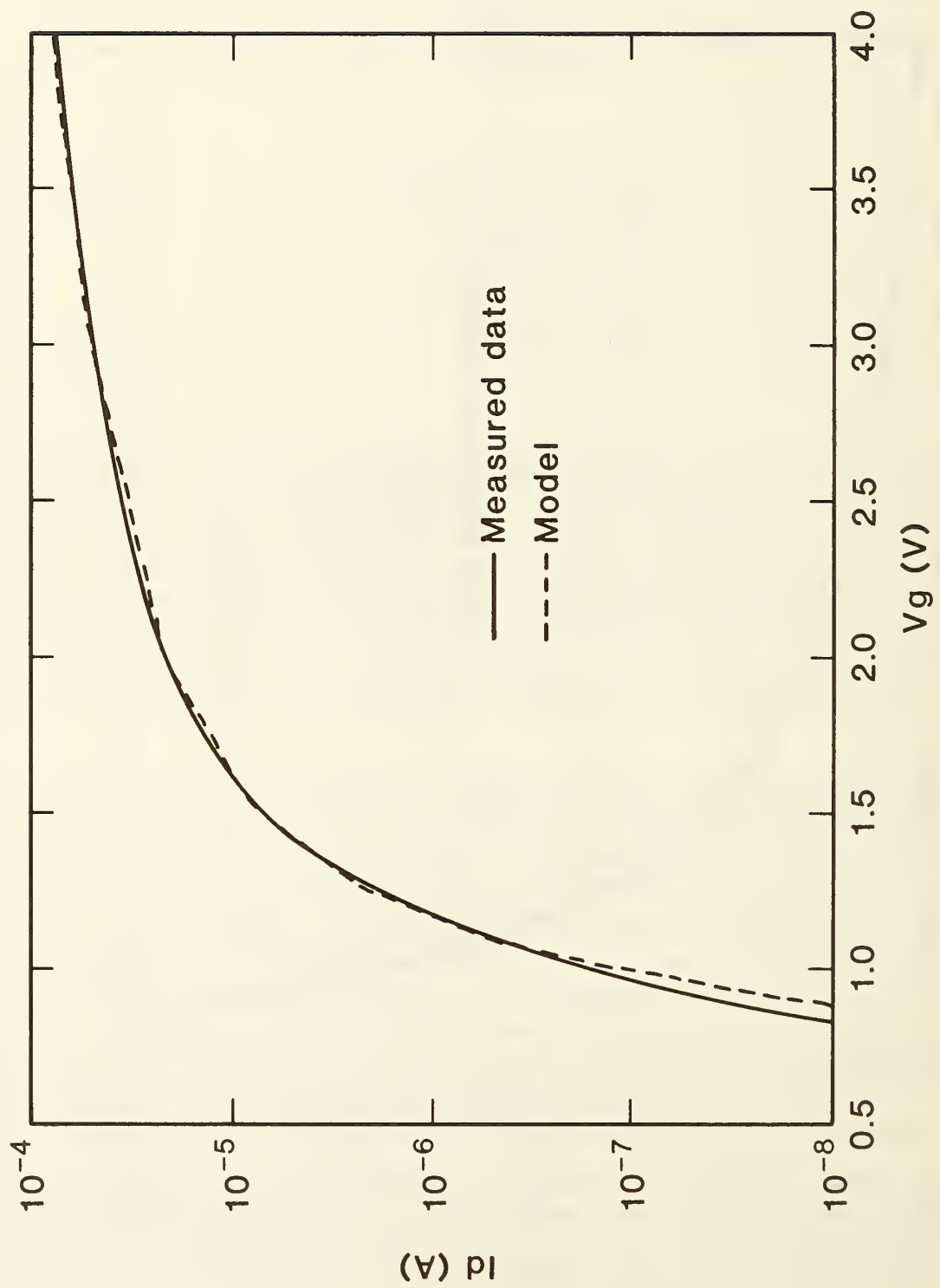


Figure 3. A subthreshold region simulation compared to measured data for a 10 Krad(Si) dose,  $V_d=0.25$  V.

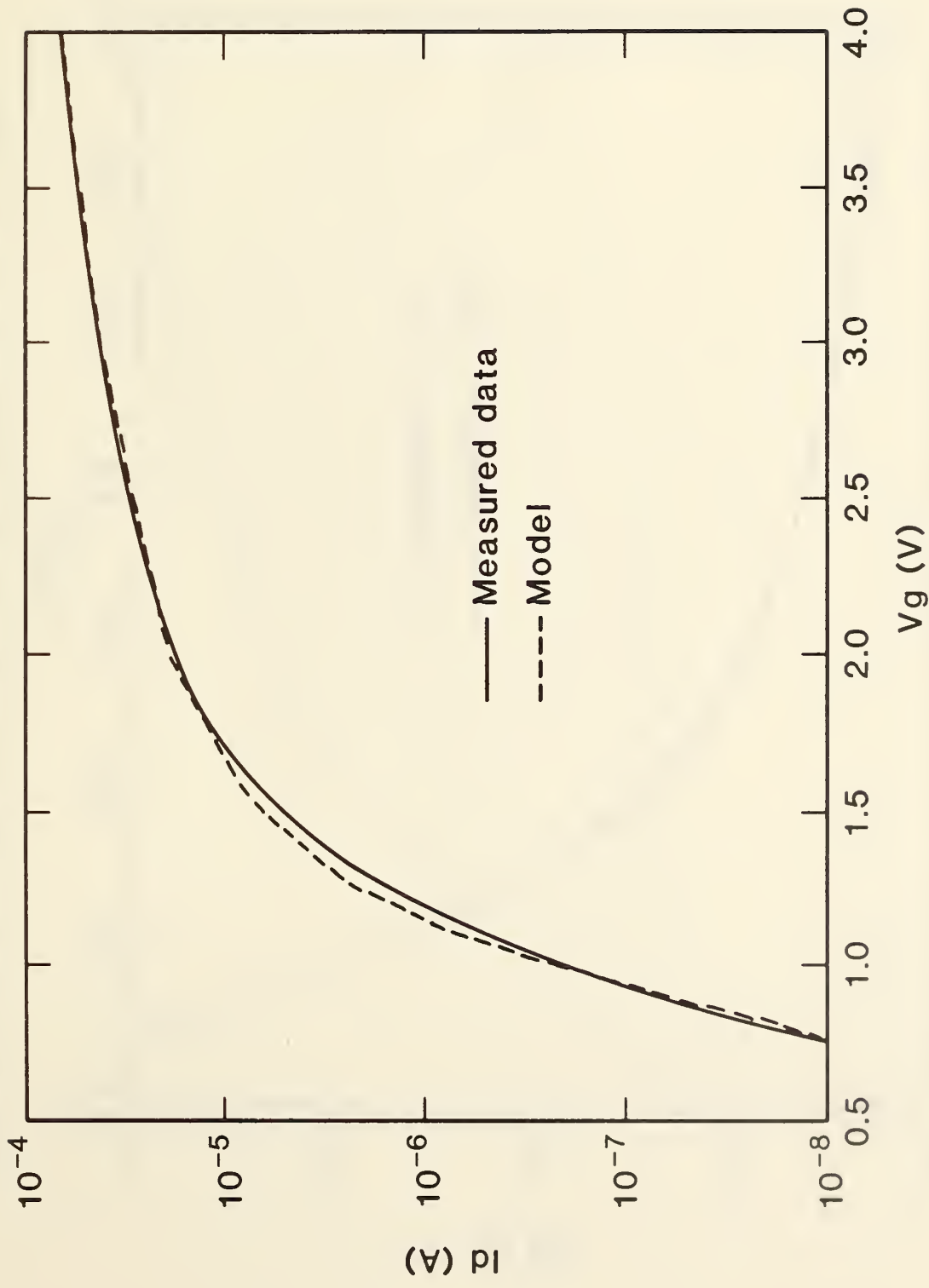


Figure 4. A subthreshold region simulation compared to measured data for a 50 Krad(Si) dose,  $V_d=0.25$  V.

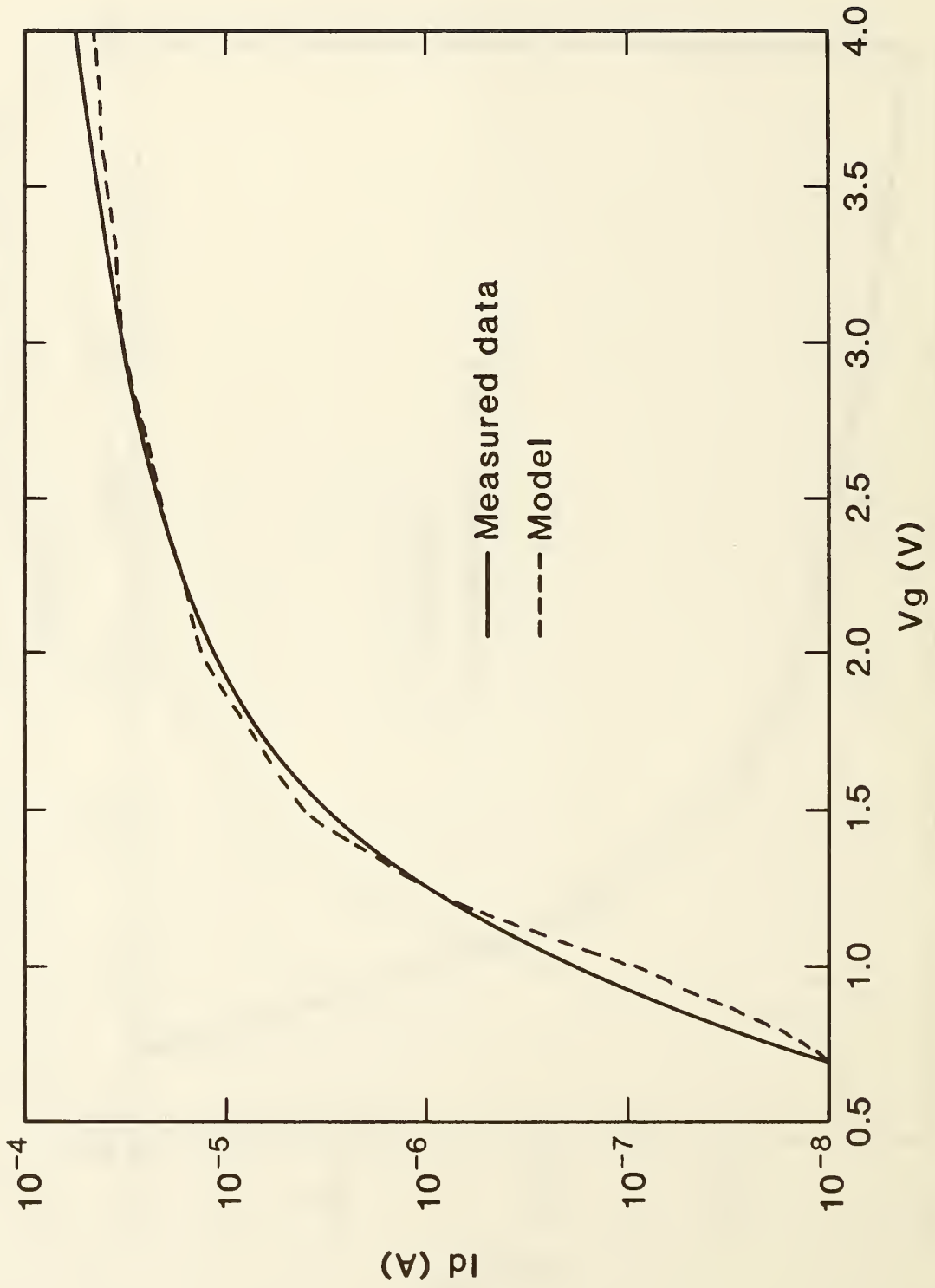


Figure 5. A subthreshold region simulation compared to measured data for a 100 Krad(Si) dose,  $V_d=0.25$  V.



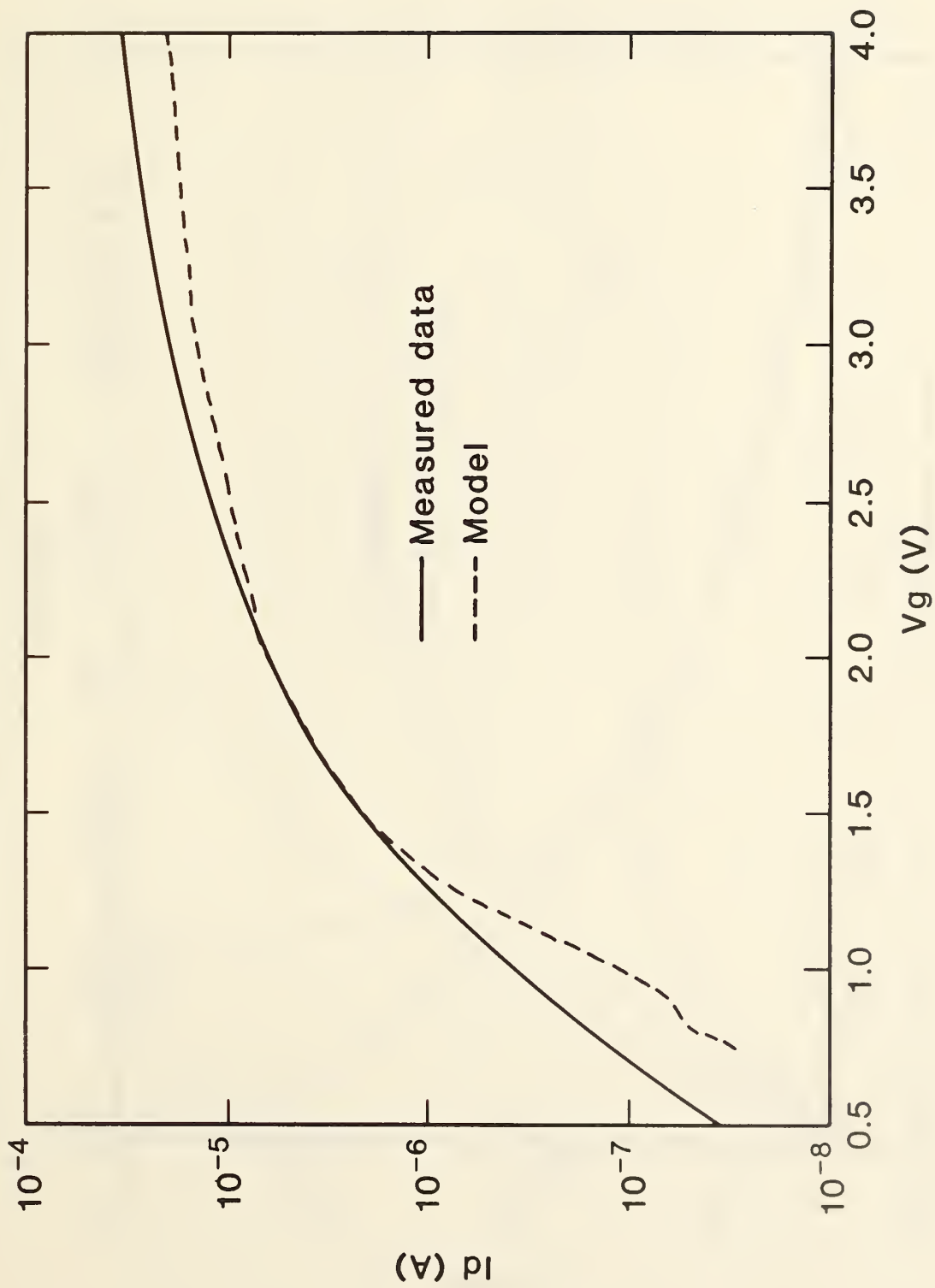


Figure 6. A subthreshold region simulation compared to measured data for a 500 Krad(Si) dose,  $V_d=0.25$  V, uniform trap distribution.

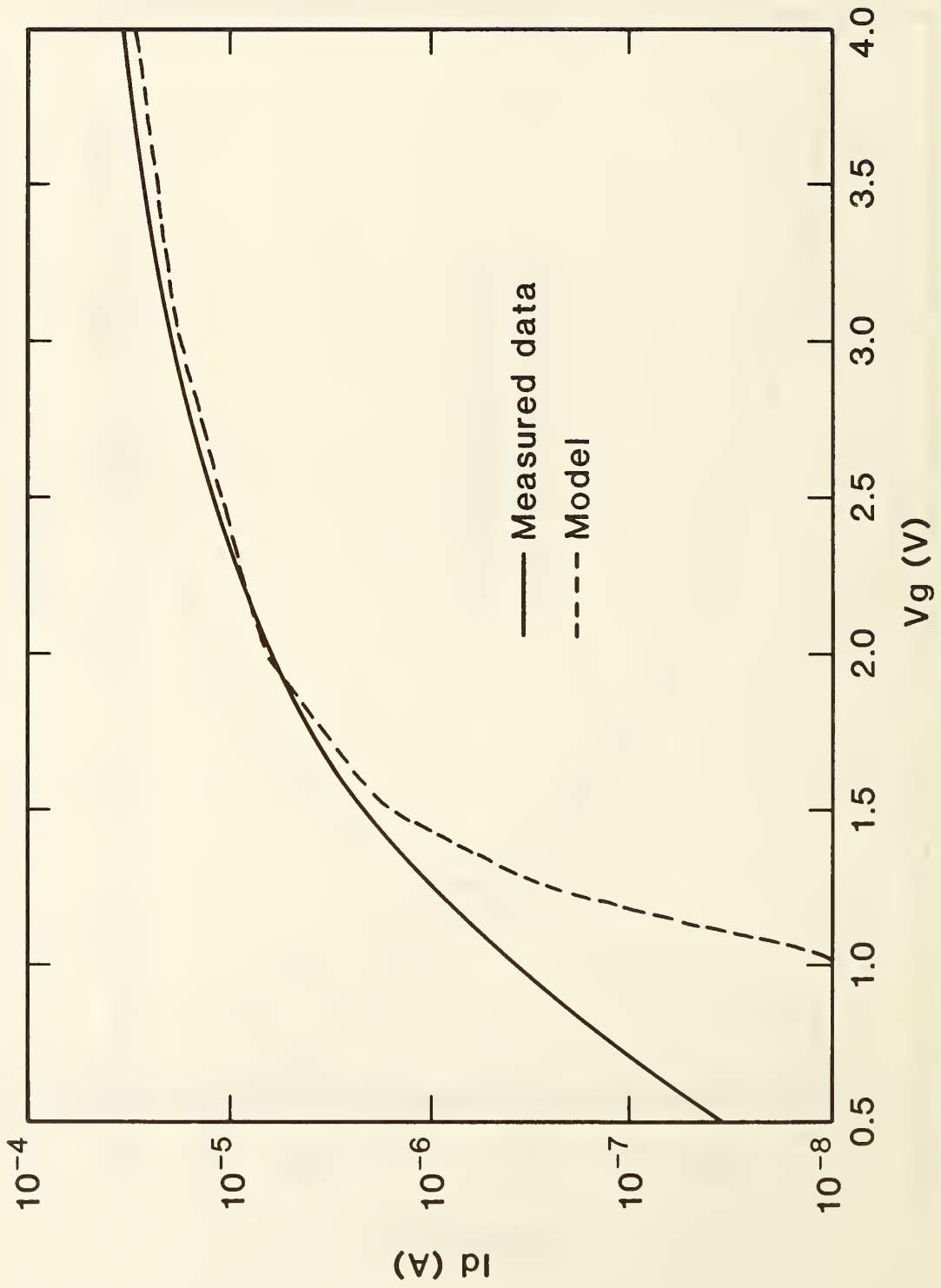


Figure 7. A subthreshold region simulation compared to measured data for a 500 Krad(Si) dose,  $V_d=0.25$  V, trap distribution peaked near the valence band.

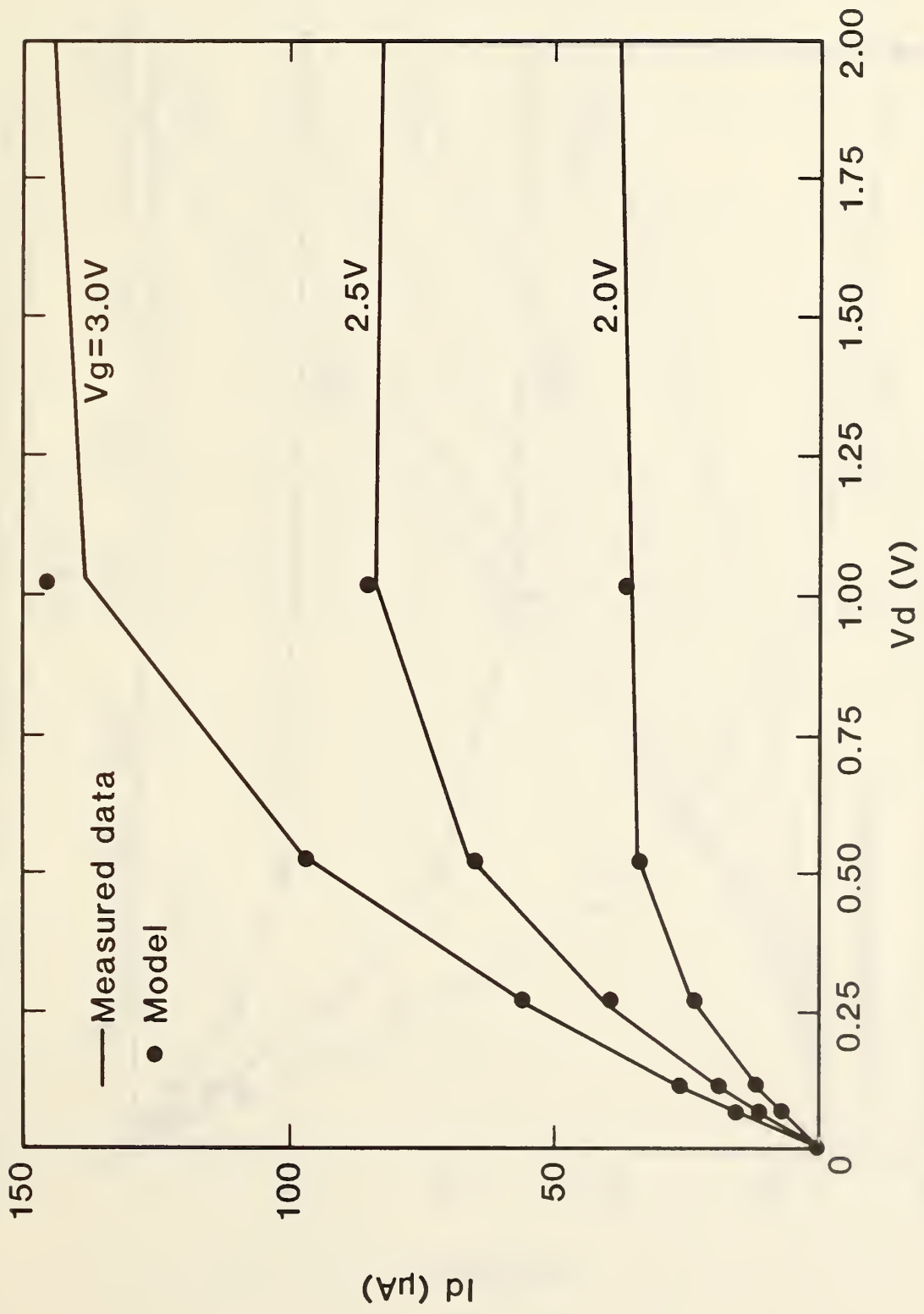


Figure 8. A saturation region simulation compared to measured data for an unirradiated transistor.

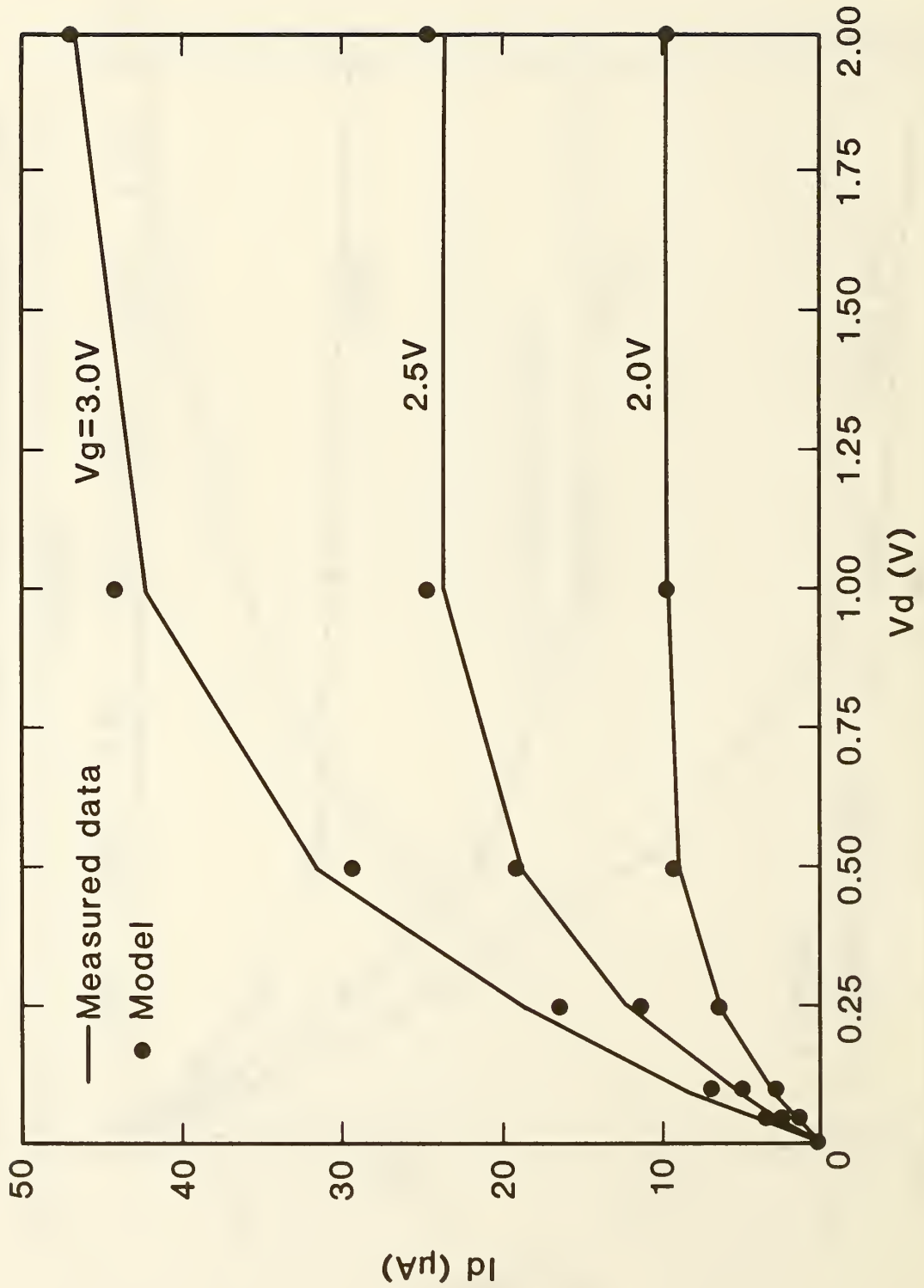


Figure 9. A saturation region simulation compared to measured data for a 500 Krad(Si) dose.

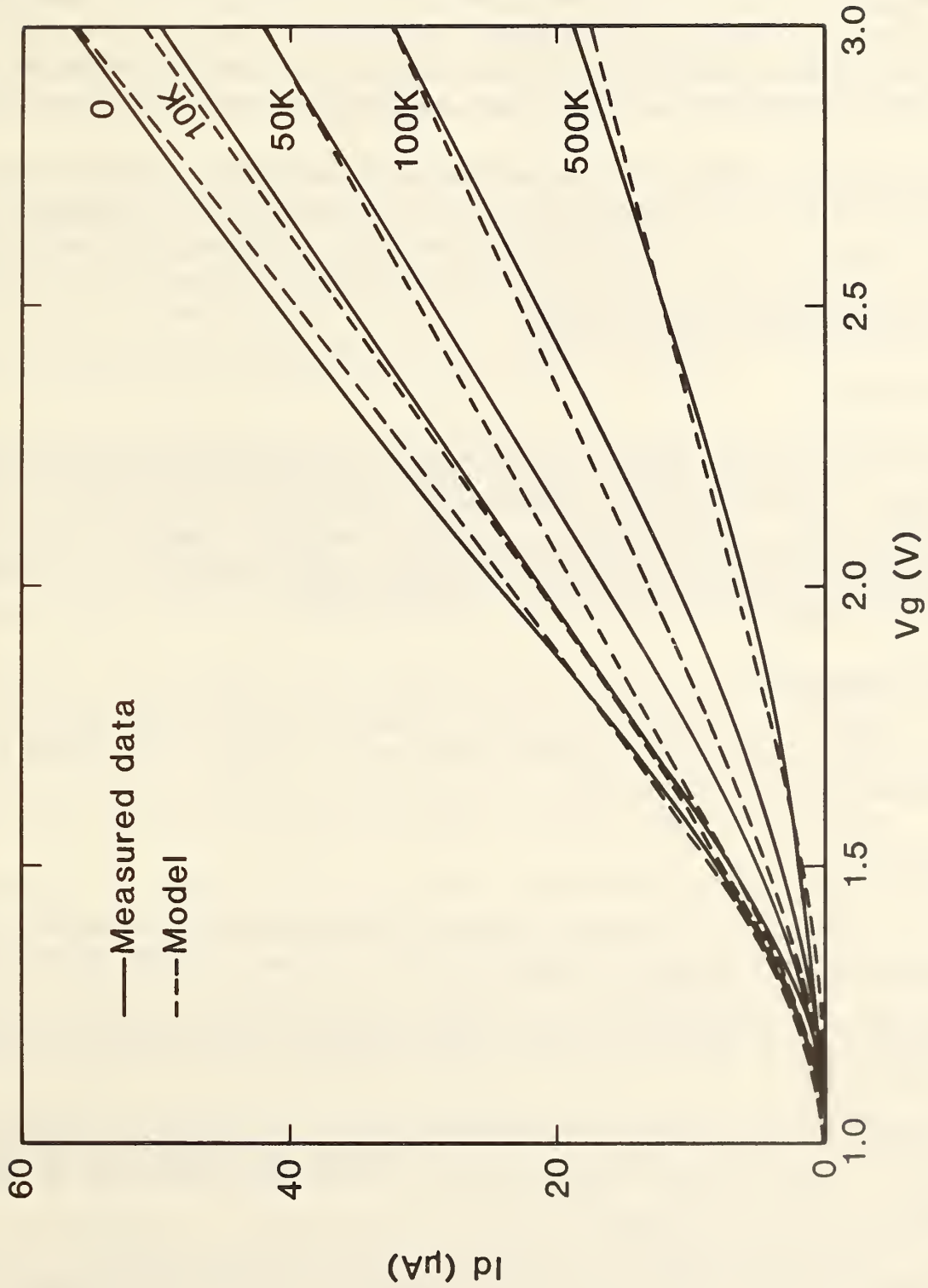


Figure 10. The triode region characteristics, as a function of dose, compared to measured data,  $V_d=0.25$  V.

produce a total threshold shift of  $\approx 0.25$  V at 500 Krad(Si). The resulting increase in interface charge causes a decrease in channel mobility from  $760 \text{ cm}^2/\text{V}\cdot\text{sec.}$  in the unirradiated device to  $257 \text{ cm}^2/\text{V}\cdot\text{sec.}$  at 500 Krad(Si). The increase in interface charge also results in an increase in subthreshold current and a decrease in subthreshold slope. Simple linear relationships between dose and both oxide charge and interface charge are sufficient to account for all of these device characteristics.

The model shows that the I-V characteristics of the heavily irradiated device are similar to those of an unirradiated device of much shorter channel length. In the short-channel device, the subthreshold characteristic is degraded by the drain field. In the irradiated device, this subthreshold degradation is caused by the charge in the radiation-induced interface traps.

## 5. Conclusions

A two-dimensional charge-sheet model of a surface-channel MOS transistor has been developed. When this model is implemented using adaptive finite element methods, an efficient high-accuracy transistor simulation program is possible. The inclusion of interface trap energy distribution allows the characteristics to be modeled for n-channel transistors for doses of up to 500 Krad(Si).

## Acknowledgments

The authors would like to thank M. Gaitan and T. J. Russell for the data used to verify the model.

## References

1. De La Moneda, F., Threshold Voltage from Numerical Solutions of the Two-Dimensional MOS Transistor, *IEEE Trans. Circuit Theory CT-20*, 666-673 (1973).
2. Brews, J. R., A Charge-Sheet Model of the MOSFET, *Solid-State Electronics* 21, 345-355 (1978).
3. Wilson, C. L., and Blue, J. L. Two-Dimensional Finite Element Charge-Sheet Model of a Short-Channel MOS Transistor, *Solid-State Electronics* 25, 461-477 (1982).
4. Wilson, C. L., and Blue, J. L., Two-Dimensional Finite Element Charge-Sheet Model of a Short-Channel MOS Transistor, National Bureau of Standards report NBSIR 82-2471 (1982).

5. Greenfield, J. A., and Dutton, R. W., Nonplanar VLSI Device Analysis Using the Solution of Poissons's Equation, *IEEE Trans. Electron Devices* ED-27, 1520-1532 (1980).
6. Selberherr, S., Schutz, A., and Potzl, H. W., MINIMOS - A Two-Dimensional MOS Transistor Analyzer, *IEEE Trans. Electron Devices* ED-27, 1540-1549 (1980).
7. Buturla, E. M., and Cottrell, P. E., Two-Dimensional Finite-Element Analysis of Semiconductor Steady-State Transport Equations, *Int. Conf. on Computational Methods in Nonlinear Mechanics*, Austin, Texas, 1974.
8. Fichtner, W., and Rose, D. J., On the Numerical Solution of Nonlinear Elliptic PDE's Arising from Semiconductor Device Modeling, *Elliptic Problem Solvers*, M. Schultz, Ed. (Academic Press, New York, 1981), pp. 277-284.
9. Bank, R. E., and Sherman, A. H., PLTMG User's Guide, CNA-152, Center for Numerical Analysis, University of Texas at Austin, September 1979.
10. Laux, S. E., and Lomax, R. I., Numerical Investigation of Mesh Size Convergence Rate of Finite Element Method in MESFET Simulation, *Solid-State Electronics* 24, 485-493 (1981).
11. Brews, J. R., Fichtner, W., Nicollian, E. H., and Sze, S. M., Generalized Guide for MOSFET Miniaturization, *Electron Device Letters* EDL-1, 2-4 (1980).
12. Wilson, C. L., and Blue, J. L., Semiconductor Device Simulation, *Elliptic Problem Solvers*, M. Schultz, Ed. (Academic Press, New York, 1981), pp. 435-439.
13. Strang, G., and Fix, G. J., *An Analysis of the Finite Element Method* (Prentice-Hall, Englewood Cliffs, N.J., 1973).
14. Eisenstat, S. C., Gursky, M. C., Schultz, M. A. and Sherman, A. H., Yale Sparse Matrix Package I. The Symmetric Codes, Research Report #112, Department of Computer Science, Yale University, 1976.
15. Brandt, A., Multi-Level Adaptive Solutions to Boundary-Value Problems, *Math. Comp.* 31, 333-390 (1977).
16. Swarztrauber, P., and Sweet, R., Efficient FORTRAN Subprograms for the Solution of Elliptic Partial Differential Equations, NCAR Technical Note, NCAR-TN/IA-109, 1975.
17. Fox, P. A., Hall, A. D., and Schryer, N. L., The PORT Mathematical Subroutine

Library, *ACM Trans. Mathematical Software* 2, 104-126 (1978).

18. Blue, J. L., Automatic Numerical Quadrature - DQUAD, Bell Labs Comput. Sci. Tech. Rep. 25, February 1975; also, Automatic Numerical Quadrature, *Bell Syst. Tech. J.* 59, 1651-1678 (1977).

19. Brent, R. P., *Algorithms for Minimization Without Derivatives* (Prentice-Hall, Englewood Cliffs, N.J., 1973), pp. 188-189.

20. Cooper, J. A., Jr., and Nelson, D. F., Measurement of High-Field Drift Velocity of Electrons in Inversion Layers on Silicon, *IEEE Electron Device Letters* EDL-2, 171-173 (1981).

21. Warner, D. D., and Wilson, C. L., Two-Dimensional Concentration Dependent Diffusion, *Bell Syst. Tech. J.* 59, 1-41 (1980).

22. Wilson, C. L., Scanning Electron Microscope Measurements on Short Channel MOS Transistors, *Solid-State Electronics* 23, 345-356 (1980).

23. Kennedy, D. P., and O'Brien, R. R., Analysis of the Impurity Atom Distribution Near the Diffusion Mask for a Planar p-n Junction, *IBM J. Res. Dev.* 9, 179-186 (1965).

24. Dressendorfer, P. V., Soden, J. M., Harrington, J. J., and Nordstrom, T. V., The Effects of Test Conditions on MOS Radiation-Hardness Results, *IEEE Trans. Nucl. Sci.* NS-28, 4281-4287 (1981).



## Appendix A File CS1R.HLP

### 1. Interactive Execution

On a VAX 11/780 the program is executed by entering:

```
RUN CS1R.EXE
```

A prompt will appear for the next input; enter a file name after each prompt, followed by a carriage return (denoted <cr>)

```
FILENAME1<cr>  
FILENAME2<cr>  
FILENAME3<cr>  
FILENAME4<cr>  
FILENAME5<cr>  
FILENAME6<cr>
```

The first and third files must have been created prior to this execution. They contain input data used by the program. The second file may be created during execution. The FILENAMEs must be legal VMS file names; they are limited to eight characters by an internal buffer in CS1R.

#### A. FILES

- 1) File1 contains data for each point to be calculated. The file format is shown below.
- 2) File2 is an empty file for output of plotting data if the plots are to be saved. This file name must be entered when if no plotting is to be done. VMS will create the file if plotting data are to be stored; other operating systems may require the file to be created before the run begins.
- 3) File3 contains a table of channel doping profiles.
- 4) File4 contains a table of acceptor trap density vs energy.
- 5) File5 contains a table of donor trap density vs energy.
- 6) File6 contains a table of oxide charge density vs distance.

#### B. Examples of FILE FORMATS.

Each point to be calculated requires 5 lines of input.

Data on a given line are free-format. Comments may appear after all required data fields. After each point

is calculated, the program will look for additional data until a source doping of zero is found (first line of input), after which the program will terminate.

EXAMPLE OF File1: Data are in units given.

Line 1:

Source doping/cm\*\*3

3.0e19

Line 2:

Vertical junction depth(um),Lateral junction depth(um),Poly-Si length(um)

note: Channel length = Poly-Si length-2\*Lateral junction depths

0.55 0.84 5.00

Line 3:

Drain(volts),Gate(volts),Substrate(volts)

note: Source voltage = 0.0.

0.15 +1.158 0.0

Line 4:

Oxide thickness(um),Oxide dielectric constant,Interface charge(cm\*\*2)

0.057 4.0 0.0

Line 5:

Channel mobility(cm\*\*2/V-sec),Channel width(um),Flatband voltage(V)

400.0 20.0 -.580

Line 6:

Line 6 may contain 0.0 for stopping program, or may be first line of data for next point to be calculated. Last line in data file must be zero.

EXAMPLE of File3: Data for doping density.

Line 1:

Contains integer, Ndop, denoting the length of the profile table.

2

Lines 2 through Ndop+1:

Each contains an x (um) and the doping density at x (1/cm\*\*3)

0.0 3.e15

100.0 3.e15

EXAMPLE of File4: Data for acceptor trap density.

Line 1:

Contains integer, Nqa, denoting the length of the table and a scale factor.

4 0.144

Lines 2 through Nqa+1:

Each contains an energy referred to mid-band (Ev) and the density 1/(Ev-cm\*\*2).

-0.500	0.0
-0.499	1.0e11
0.499	1.0e11
0.500	0.0

EXAMPLE of File5: Data for donor trap density.

Line 1:

Contains integer, Nqd, denoting the length of the table and a scale factor.

4 0.144

Lines 2 through Nqd+1:

Each contains an energy referred to mid-band (Ev) and the density 1/(Ev-cm\*\*2).

-0.500	0.0
-0.499	1.0e11
0.499	1.0e11
0.500	0.0

EXAMPLE of File6: Data for oxide charge density.

Line 1:

Contains integer, Nqox, denoting the length of the table and a scale factor.

4 1.00

Lines 2 through Nqox+1:

Each contains a distance referred to the source (um) and the density 1/(cm\*\*2).

0.000	0.0
0.100	1.0e11
5.000	1.0e11
5.500	0.0

### C. OUTPUT DISPLAY

All outputs (except the drain current) are in intrinsic Debye lengths (33um) and thermal volts (25mV), or units derived from these such as, Thermal volts/Debye length.

1. After program execution, the following prompts appear on the display:

ENTER 0,1,2,3 FOR CURRENT AND NEXT POINT, 2D PRINTING,  
2D PLOTTING, CURRENT AND STOPPING.

- 0 – print current. Continue to next point in data file, if any.
- 1 – print additional information about point just calculated.
- 2 – plot additional information about point just calculated.
- 3 – print current and terminate execution. Do not continue to next data point in data file, if any.

If response 1 or 2 is given, further prompts will be furnished.

2. OPTIONS for printing (response 1)

The prompt is

ENTER SUMMARY,NX,NY

SUMMARY – for a summary of the number of mesh points and triangles

created, how much memory allocated, and how much time used, enter 1. If not desired, enter 0.

NX NY – how many points along X and Y are to be printed in the print matrix. If NX and NY are both negative, a scaled integer printer plot of the potential will result. If NX and NY are both positive, a rectangular grid is placed on the region; at each point X, Y, U (the potential), UX, and UY (the derivatives of U in the X and Y directions) will be printed. At grid points outside the region, large numbers will be printed.

3. OPTIONS for plotting (response 2)

The prompt is

1:TRIANGLES, 2:CONTOURS, 3:SURFACE, 4:PROFILES

Enter 1, 2, 3, or 4, to plot on screen.

Enter 101, 102, 103, or 104, to save plot data on File2.

Enter 0 to terminate plotting.

Each plot mode will furnish one or more further prompts. In every screen-plotting case, the final prompt before drawing the plot is

Enter g or G to when ready to plot

This gives the user time to clear the screen or to do any work necessary to put the terminal in plotting mode.

After each plot is drawn on the screen, the program will wait for a carriage return, and then re-issue the above prompt. This gives the user time to clear the screen or to do any work necessary to change the terminal out of plotting mode.

## 1: TRIANGLE PLOTS

The prompt is  
ENTER LEVEL

Enter level number (1, 2, ...) to plot the mesh of that level.  
Enter 0 to terminate triangle plotting.

After the triangle plot has been drawn, the program waits for a carriage return, and then reissues the Triangle Plot prompt.

## 2: CONTOUR PLOTS

The first prompt is  
1:FUNCTION, 2:ABS(GRADIANT)

Enter 1 to plot the function (potential), or 2 to plot the absolute value of its gradient (absolute value of electric field; units are thermal volts/Debye length).

Enter 0 to terminate contour plotting.

The next prompt is  
NUMBER OF CONTOURS

Enter the number of contour lines to be drawn. They will be drawn equally-spaced between (and including) the minimum and maximum values found.

After the contour plot has been drawn, the program waits for a carriage return, and then reissues the first Contour Plot prompt.

### 3: SURFACE PLOTS

The first prompt is  
1:FUNCTION, 2:ABS(GRADIENT)

Enter 1 to plot the function (potential), or 2 to plot the absolute value of its gradient (absolute value of electric field; units are thermal volts/Debye length).

Enter 0 to terminate surface plotting.

The next prompt is  
ENTER LEVEL

Enter level number (1, 2, ...) to make a plot of the surface using the mesh of the given level.

Enter 0 to return to the First Surface Plot prompt

The next prompt is  
ENTER VIEWING DIRECTION-NX,NY,NZ

Enter three integers. The surface plot is a (parallel) projection of the surface as seen from indicated direction. Thus (0,0,1) will give a top view (like a Triangle Plot), and (0,-1,0) will give a side view.

After the surface plot has been drawn, the program waits for a carriage return, and then reissues the first Surface Plot prompt.

### 4: PROFILE PLOTS

The first prompt is  
ENTER NUMBER OF PROFILES

Enter an integer, the number of profiles to be drawn.

Enter 0 to terminate profile plotting.

The next prompt is

ENTER INDICES OF PROFILE PLANE(S), NX AND NY

Enter two integers. A profile plot is a slice through the solution, perpendicular to the given direction. Thus (0,1) will give a slice parallel to the X axis.

After the profile plot has been drawn, the program waits for a carriage return, and then reissues the first Profile Plot prompt.

## 2. BATCH EXECUTION (for VAX-VMS only)

### A. Submit File

Create a submit file which contains:

```
$ RUN CS1R.EXE  
FILENAME1  
FILENAME2  
FILENAME3  
FILENAME4  
FILENAME5  
FILENAME6
```

(Any other input used for the the equivalent interactive execution).

B. Output will be printed on the line printer.

## 3. SUMMARY OF MODEL

A two-dimensional charge sheet model of a surface-channel MOS transistor has been developed. When this model is implemented using adaptive finite element methods, an efficient high-accuracy transistor simulation program is possible.

The primary effect of ionizing radiation on MOSFETs is the

introduction of oxide trapped charge (OTC) and interface trapped charge (ITC). The OTC is independent of device operating voltage after irradiation, while the charge state of the ITC is dependent on gate bias in the subthreshold and weak inversion regions. Inclusion of these two charge components in device models introduces a nonscalable component into the calculation of the total effective channel charge in short-channel transistors.



Appendix B  
File CS1R.EXP

INPUT FILE NAME FOR INPUT DATA,  
FILE specification MUST BE <= 40 CHARACTERS.

s8.dat (user input)

INPUT FILE NAME FOR OUTPUT DATA PLOTTING

plot.dat (user input)

INPUT FILENAME FOR DOPING PROFILE DATA

dops8.dat (user input)

INPUT FILENAME FOR QIA ENERGY DATA

qa.dat (user input)

INPUT FILENAME FOR QID ENERGY DATA

qd.dat (user input)

INPUT FILE NAME FOR QOX VS DISTANCE DATA

qox.dat (user input)

BETA = 3.868472E+01  
 PSIB = 3.466497E-01  
 LB = 4.086666E-06  
 COX = 6.207734E-08  
 BPSO = 2.331485E+01  
 BPSI = 3.318985E+01  
 PS(O) = 8.579575E-01  
 NO = 1.106634E+12  
 PS(L) = 1.104439E+00  
 NL = 9.657040E+11  
 ID = 8.584329E-05  
 IO = 5.349826E+01  
 I... = 9.999379E+02  
 VG = 1.547389E+02  
 VSD = 9.671180E+00  
 LCH = 2.481457E-01

level 1

1	dpsi	-1.553E+01	a	-2.540E+08	umax	4.639E+01
2	dpsi	9.854E+00	a	-1.500E+08	umax	1.042E+01
3	dpsi	4.886E+00	a	-1.088E+08	umax	1.042E+01
4	dpsi	8.537E+00	a	-9.717E+07	umax	8.693E+00
5	dpsi	8.361E+00	a	-1.199E+08	umax	8.575E+00
6	dpsi	4.273E+00	a	-1.731E+08	umax	4.311E+00
7	dpsi	2.256E+00	a	-2.395E+08	umax	2.277E+00
8	dpsi	1.012E+00	a	-3.043E+08	umax	1.016E+00

9	dpsi	-8.973E-01	a	-3.470E+08	umax	9.037E-01
10	dpsi	-8.854E-01	a	-3.421E+08	umax	8.919E-01
11	dpsi	-8.539E-01	a	-2.968E+08	umax	8.614E-01
12	dpsi	-7.848E-01	a	-2.413E+08	umax	7.944E-01
13	dpsi	-6.455E-01	a	-1.945E+08	umax	6.582E-01
14	dpsi	-4.437E-01	a	-1.631E+08	umax	4.455E-01
15	dpsi	4.279E-01	a	-1.538E+08	umax	4.455E-01

level 2

1	dpsi	7.609E-02	a	-1.529E+08	umax	4.455E-01
2	dpsi	1.169E+00	a	-1.408E+08	umax	2.663E+01
3	dpsi	1.234E+00	a	-1.366E+08	umax	1.977E+01
4	dpsi	3.674E+00	a	-1.372E+08	umax	1.429E+01
5	dpsi	2.572E+00	a	-1.846E+08	umax	2.737E+00
6	dpsi	2.915E-01	a	-1.920E+08	umax	1.188E+00
7	dpsi	2.092E-01	a	-1.994E+08	umax	1.064E+00
8	dpsi	2.829E-03	a	-1.996E+08	umax	1.057E+00

level 3

1	dpsi	4.082E-04	a	-1.996E+08	umax	1.057E+00
2	dpsi	7.940E-01	a	-2.113E+08	umax	7.997E+00
3	dpsi	5.418E-01	a	-2.552E+08	umax	1.191E+00
4	dpsi	-2.892E-01	a	-2.826E+08	umax	9.930E-01
5	dpsi	-2.685E-01	a	-2.875E+08	umax	5.127E-01
6	dpsi	-2.579E-01	a	-2.772E+08	umax	2.583E-01

ENTER 0 FOR CURRENT AND NEXTPOINT

- 1 FOR 2D PRINTING
- 2 FOR 2D PLOTTING
- 3 FOR CURRENT AND STOPPING
- 4 FOR CHANNEL PRINTING

1 (user input)

enter summary, nx, ny

1 -6 -11 (user input)

### 3 MULTI-GRID LEVELS

VERTICES	146	340	517
TRIANGLES	322	852	1344

STORAGE ALLOCATION

	ALLOCATED	USED
MAXT	17655	1349
MAXV	6621	517
MAXVSM	8828	1006
MAXJA	35877	3766
MAXU	1099	1099
MAXJU	1099	1062
TOTAL	200000	19992

TIMING DISTRIBUTION

	SECONDS	PERCENT
GRID	0.540	0.298
ASMBLY	133.740	73.784
MG	38.620	21.306
ADAPT	8.360	4.612
TOTAL	181.260	100.000

scaled values from -1.410E+01 to 3.344E+01 scale 3.344E+01

```

9999 9999 -39 -41 -40 -38
9999 9999 -42 -41 -40 -38
 100 -42 -42 -41 -40 -38
   96 -42 -42 -41 -40 -38
   92 -42 -42 -41 -40 -38
   88 -42 -42 -41 -40 -38
   85 -42 -42 -41 -40 -38
   81 -42 -42 -41 -40 -38
   77 -42 -42 -41 -40 -38
9999 9999 -42 -41 -40 -38
9999 9999 -41 -41 -40 -38

```

ENTER 0 FOR CURRENT AND NEXTPOINT

1 FOR 2D PRINTING

2 FOR 2D PLOTTING

3 FOR CURRENT AND STOPPING

4 FOR CHANNEL PRINTING

1 (user input)

enter summary,nx,ny

0 6 11 (user input)

I X Y U UX UY

1	0.00000	0.00000	1.70141E+38	1.70141E+38	1.70141E+38
2	0.01716	0.00000	1.70141E+38	1.70141E+38	1.70141E+38
3	0.03432	0.00000	-1.37603E+01	-1.15893E+01	-1.00326E+02
4	0.05148	0.00000	-1.35980E+01	2.32617E+01	-2.00069E+00
5	0.06864	0.00000	-1.32181E+01	2.17328E+01	-3.08984E-01
6	0.08580	0.00000	-1.28544E+01	2.11106E+01	-2.26113E-01
7	0.00000	0.03333	1.70141E+38	1.70141E+38	1.70141E+38
8	0.01716	0.03333	1.70141E+38	1.70141E+38	1.70141E+38
9	0.03432	0.03333	-1.40133E+01	3.47357E+01	-2.64253E+00
10	0.05148	0.03333	-1.36049E+01	2.32352E+01	-3.97550E-02
11	0.06864	0.03333	-1.32227E+01	2.20039E+01	6.71393E-02
12	0.08580	0.03333	-1.28544E+01	2.13377E+01	0.00000E+00
13	0.00000	0.06665	2.56068E+01	-7.69545E+03	6.86773E+01
14	0.01716	0.06665	-1.41004E+01	-1.64209E+00	8.90639E-01
15	0.03432	0.06665	-1.40099E+01	2.69803E+01	-6.98656E-01
16	0.05148	0.06665	-1.36036E+01	2.29632E+01	1.84883E-02
17	0.06864	0.06665	-1.32223E+01	2.19542E+01	-1.14683E-02
18	0.08580	0.06665	-1.28545E+01	2.13854E+01	0.00000E+00
19	0.00000	0.09998	2.71429E+01	-7.79302E+03	9.72625E+01
20	0.01716	0.09998	-1.40999E+01	4.87984E+00	-1.99454E-01
21	0.03432	0.09998	-1.39963E+01	1.53671E+01	1.52627E+00
22	0.05148	0.09998	-1.36035E+01	2.28412E+01	1.19908E-02
23	0.06864	0.09998	-1.32227E+01	2.19542E+01	-1.14683E-02
24	0.08580	0.09998	-1.28545E+01	2.13854E+01	0.00000E+00
25	0.00000	0.13330	2.83510E+01	-8.25570E+03	1.48578E+01
26	0.01716	0.13330	-1.40893E+01	-5.37798E+00	5.95635E-01
27	0.03432	0.13330	-1.39811E+01	1.67567E+01	-5.16155E+00
28	0.05148	0.13330	-1.36031E+01	2.28756E+01	1.81705E-02
29	0.06864	0.13330	-1.32229E+01	2.18015E+01	-1.84935E-02
30	0.08580	0.13330	-1.28544E+01	2.14624E+01	0.00000E+00
31	0.00000	0.16663	2.95216E+01	-8.13601E+03	4.19888E+01
32	0.01716	0.16663	-1.40986E+01	-6.38180E+00	-4.97834E-01
33	0.03432	0.16663	-1.39721E+01	1.73758E+01	6.77655E+00
34	0.05148	0.16663	-1.36069E+01	2.38427E+01	-5.01812E-01
35	0.06864	0.16663	-1.32235E+01	2.18015E+01	-1.84935E-02
36	0.08580	0.16663	-1.28544E+01	2.14624E+01	0.00000E+00
37	0.00000	0.19996	3.06777E+01	-8.50732E+03	4.61548E+01
38	0.01716	0.19996	-1.40893E+01	-4.21487E+00	5.42349E-02
39	0.03432	0.19996	-1.39811E+01	1.67966E+01	5.21157E+00
40	0.05148	0.19996	-1.36031E+01	2.28729E+01	-1.87395E-02
41	0.06864	0.19996	-1.32229E+01	2.18015E+01	1.87087E-02

42	0.08580	0.19996	-1.28544E+01	2.14624E+01	0.00000E+00
43	0.00000	0.23328	3.19591E+01	-8.33355E+03	2.53904E+01
44	0.01716	0.23328	-1.41009E+01	1.41400E+01	1.46553E+00
45	0.03432	0.23328	-1.39964E+01	1.55038E+01	-1.51089E+00
46	0.05148	0.23328	-1.36036E+01	2.28469E+01	-1.40815E-02
47	0.06864	0.23328	-1.32227E+01	2.19575E+01	1.05458E-02
48	0.08580	0.23328	-1.28544E+01	2.13845E+01	0.00000E+00
49	0.00000	0.26661	3.34385E+01	-8.54575E+03	1.13276E+02
50	0.01716	0.26661	-1.40937E+01	-2.87519E+00	-7.03582E-01
51	0.03432	0.26661	-1.40099E+01	2.75868E+01	5.18849E-01
52	0.05148	0.26661	-1.36035E+01	2.29437E+01	-5.59664E-03
53	0.06864	0.26661	-1.32223E+01	2.19575E+01	1.05458E-02
54	0.08580	0.26661	-1.28544E+01	2.13845E+01	0.00000E+00
55	0.00000	0.29993	1.70141E+38	1.70141E+38	1.70141E+38
56	0.01716	0.29993	1.70141E+38	1.70141E+38	1.70141E+38
57	0.03432	0.29993	-1.40225E+01	4.93789E+01	7.53808E+00
58	0.05148	0.29993	-1.36073E+01	2.36961E+01	-2.07513E-02
59	0.06864	0.29993	-1.32227E+01	2.19793E+01	-6.87528E-02
60	0.08580	0.29993	-1.28544E+01	2.13406E+01	0.00000E+00
61	0.00000	0.33326	1.70141E+38	1.70141E+38	1.70141E+38
62	0.01716	0.33326	1.70141E+38	1.70141E+38	1.70141E+38
63	0.03432	0.33326	-1.29085E+01	-3.49977E+02	2.29821E+02
64	0.05148	0.33326	-1.36006E+01	2.27103E+01	-3.52586E-01
65	0.06864	0.33326	-1.32178E+01	2.21573E+01	1.15992E-01
66	0.08580	0.33326	-1.28544E+01	2.10266E+01	2.88546E-01

ENTER 0 FOR CURRENT AND NEXTPOINT

1 FOR 2D PRINTING

2 FOR 2D PLOTTING

3 FOR CURRENT AND STOPPING

4 FOR CHANNEL PRINTING

2 (user input)

1:triangles, 2:contours, 3:surface, 4:profiles

101 (user input)

writing co-ordinates instead of plotting

enter level

1 (user input)

writing to file 21 (see figure B-1)

enter level

2 (user input)

writing to file 21 (see figure B-2)

enter level

```

3                (user input)
writing to file 21 (see figure B-3)
enter level
0                (user input)
1:triangles, 2:contours, 3:surface, 4:profiles
0                (user input)
writing co-ordinates instead of plotting
103             (user input)
1:function, 2:abs(gradient)
1                (user input)
enter level
1                (user input)
enter viewing direction -- nx,ny,nz
3 -1 1          (user input)
writing to file 21 (see figure B-4)
1:function, 2:abs(gradient)
1                (user input)
enter level
2                (user input)
enter viewing direction -- nx,ny,nz
3 -1 1          (user input)
writing to file 21 (see figure B-5)
1:function, 2:abs(gradient)
1                (user input)
enter level
3                (user input)
enter viewing direction -- nx,ny,nz
3 -1 1          (user input)
writing to file 21 (see figure B-6)
1:function, 2:abs(gradient)
0                (user input)
1:triangles, 2:contours, 3:surface, 4:profiles
102            (user input)
writing co-ordinates instead of plotting
1:function, 2:abs(gradient)
1                (user input)
number of contours
-8              (user input)
umin and umax
-10 25          (user input)
ulev

```

-1.000E+01 -5.000E+00 0.000E+00 5.000E+00 1.000E+01  
1.500E+01 2.000E+01 2.500E+01

writing to file 21 (see figure B-7)

1:function, 2:abs(gradient)

0 (user input)

1:triangles, 2:contours, 3:surface, 4:profiles

0 (user input)

ENTER 0 FOR CURRENT AND NEXTPOINT

1 FOR 2D PRINTING

2 FOR 2D PLOTTING

3 FOR CURRENT AND STOPPING

4 FOR CHANNEL PRINTING

0 (user input)

Vg = 4.000 Vd = 0.250 Vfb = -0.560 Q = 0.0000E+00 current 9.7684E-05

BETA = 3.868472E+01

PSIB = 3.466497E-01

LB = 4.086666E-06

COX = 6.207734E-08

BPSO = 2.331485E+01

BPSI = 3.252674E+01

PS(O) = 8.408164E-01

NO = 7.291709E+11

PS(L) = 1.085300E+00

NL = 5.889478E+11

ID = 5.458326E-05

IO = 5.349826E+01

I... = 6.358082E+02

VG = 1.160542E+02

VSD = 9.671180E+00

LCH = 2.481457E-01

level 1

1	dpsi	-1.479E+01	a	-2.528E+08	umax	4.839E+01
2	dpsi	5.689E+00	a	-1.358E+08	umax	7.711E+00
3	dpsi	5.550E+00	a	-8.503E+07	umax	7.711E+00
4	dpsi	7.272E+00	a	-6.459E+07	umax	7.478E+00
5	dpsi	5.560E+00	a	-6.957E+07	umax	5.711E+00
6	dpsi	1.788E-02	a	-6.970E+07	umax	4.878E+00
7	dpsi	1.779E-02	a	-6.983E+07	umax	4.853E+00
8	dpsi	1.768E-02	a	-6.998E+07	umax	4.828E+00
9	dpsi	1.759E-02	a	-7.009E+07	umax	4.803E+00

10	dpsi	1.749E-02	a	-7.022E+07	umax	4.578E+00
11	dpsi	1.739E-02	a	-7.035E+07	umax	4.552E+00
12	dpsi	4.428E+00	a	-9.768E+07	umax	4.527E+00
13	dpsi	2.440E+00	a	-1.370E+08	umax	2.482E+00
14	dpsi	1.050E+00	a	-1.765E+08	umax	1.058E+00
15	dpsi	-5.859E-01	a	-2.047E+08	umax	5.868E-01

level 2

1	dpsi	2.937E-02	a	-2.033E+08	umax	5.868E-01
2	dpsi	3.419E-01	a	-1.896E+08	umax	2.649E+01
3	dpsi	3.657E-01	a	-1.829E+08	umax	1.966E+01
4	dpsi	3.425E-01	a	-1.795E+08	umax	1.420E+01
5	dpsi	2.933E-01	a	-1.777E+08	umax	9.663E+00
6	dpsi	9.516E-01	a	-1.721E+08	umax	6.125E+00
7	dpsi	-4.338E-01	a	-1.653E+08	umax	1.003E+00
8	dpsi	3.321E-01	a	-1.504E+08	umax	7.332E-01
9	dpsi	3.251E-01	a	-1.405E+08	umax	3.254E-01

level 3

1	dpsi	1.507E-02	a	-1.402E+08	umax	3.254E-01
2	dpsi	4.210E-01	a	-1.275E+08	umax	8.837E+00
3	dpsi	4.559E-01	a	-1.400E+08	umax	7.946E-01
4	dpsi	2.663E-01	a	-1.507E+08	umax	2.676E-01

ENTER 0 FOR CURRENT AND NEXTPOINT

1 FOR 2D PRINTING

2 FOR 2D PLOTTING

3 FOR CURRENT AND STOPPING

4 FOR CHANNEL PRINTING

1 (user input)

enter summary, nx, ny

1 11 11 (user input)

### 3 MULTI-GRID LEVELS

VERTICES	146	342	726
TRIANGLES	322	858	1900

### STORAGE ALLOCATION

	ALLOCATED	USED
MAXT	17655	1905
MAXV	6621	720
MAXVSM	8828	1217
MAXJA	35877	4595



MAXU	1099	1099
MAXJU	1099	1062
TOTAL	200000	25205

TIMING DISTRIBUTION

	SECONDS	PERCENT
GRID	0.500	0.330
ASMBLY	108.470	71.635
MG	33.500	22.124
ADAPT	8.950	5.911
TOTAL	151.420	100.000

I	X	Y	U	UX	UY
1	0.00000	0.00000	1.70141E+38	1.70141E+38	1.70141E+38
2	0.00858	0.00000	1.70141E+38	1.70141E+38	1.70141E+38
3	0.01716	0.00000	1.70141E+38	1.70141E+38	1.70141E+38
4	0.02574	0.00000	1.70141E+38	1.70141E+38	1.70141E+38
5	0.03432	0.00000	-1.37152E+01	-7.24994E+01	-9.86443E+01
6	0.04290	0.00000	-1.37948E+01	2.27971E+01	-1.43763E+00
7	0.05148	0.00000	-1.35992E+01	2.27971E+01	-1.43763E+00
8	0.06006	0.00000	-1.34068E+01	2.20188E+01	-1.99132E-01
9	0.06864	0.00000	-1.32178E+01	2.20188E+01	-1.99132E-01
10	0.07722	0.00000	-1.30350E+01	2.10478E+01	-2.70350E-01
11	0.08580	0.00000	-1.28544E+01	2.10478E+01	-2.70350E-01
12	0.00000	0.03333	1.70141E+38	1.70141E+38	1.70141E+38
13	0.00858	0.03333	1.70141E+38	1.70141E+38	1.70141E+38
14	0.01716	0.03333	1.70141E+38	1.70141E+38	1.70141E+38
15	0.02574	0.03333	-4.80514E+00	-3.49964E+03	-2.41980E+03
16	0.03432	0.03333	-1.40162E+01	3.50974E+01	6.71809E-02
17	0.04290	0.03333	-1.38026E+01	2.25781E+01	1.41791E-02
18	0.05148	0.03333	-1.36063E+01	2.34576E+01	1.62690E-02
19	0.06006	0.03333	-1.34112E+01	2.19170E+01	1.62705E-02
20	0.06864	0.03333	-1.32227E+01	2.19880E+01	6.59292E-02
21	0.07722	0.03333	-1.30376E+01	2.14340E+01	6.59292E-02
22	0.08580	0.03333	-1.28544E+01	2.13398E+01	0.00000E+00
23	0.00000	0.06665	2.49507E+01	-7.58698E+03	5.04481E+01
24	0.00858	0.06665	-1.36085E+01	-1.46068E+02	3.19051E+01
25	0.01716	0.06665	-1.41009E+01	-1.58318E+00	8.35297E-01
26	0.02574	0.06665	-1.41098E+01	1.00770E+01	-3.55419E-01
27	0.03432	0.06665	-1.40100E+01	2.70126E+01	-6.84067E-01
28	0.04290	0.06665	-1.38036E+01	2.67176E+01	4.96515E-01

29	0.05148	0.06665	-1.36036E+01	2.29500E+01	1.03107E-02
30	0.06006	0.06665	-1.34109E+01	2.19880E+01	-3.18217E-03
31	0.06864	0.06665	-1.32223E+01	2.19563E+01	-1.07920E-02
32	0.07722	0.06665	-1.30378E+01	2.13398E+01	-1.07920E-02
33	0.08580	0.06665	-1.28545E+01	2.13848E+01	0.00000E+00
34	0.00000	0.09998	2.62073E+01	-7.72841E+03	4.12046E+01
35	0.00858	0.09998	-1.34399E+01	-1.46998E+03	1.20562E+02
36	0.01716	0.09998	-1.40998E+01	3.50989E+00	2.51406E-01
37	0.02574	0.09998	-1.41165E+01	-3.06538E+00	-2.80862E-01
38	0.03432	0.09998	-1.39963E+01	1.53389E+01	1.53542E+00
39	0.04290	0.09998	-1.38064E+01	2.29145E+01	-5.82507E-01
40	0.05148	0.09998	-1.36036E+01	2.28447E+01	1.29900E-02
41	0.06006	0.09998	-1.34111E+01	2.19563E+01	-1.07920E-02
42	0.06864	0.09998	-1.32227E+01	2.19563E+01	-1.07920E-02
43	0.07722	0.09998	-1.30379E+01	2.13848E+01	0.00000E+00
44	0.08580	0.09998	-1.28545E+01	2.13848E+01	0.00000E+00
45	0.00000	0.13330	2.75698E+01	-8.06315E+03	4.27771E+01
46	0.00858	0.13330	-1.32443E+01	-4.95397E+02	1.86663E+00
47	0.01716	0.13330	-1.40925E+01	-2.57716E+00	-6.32129E-01
48	0.02574	0.13330	-1.41251E+01	1.67888E+01	-5.20889E+00
49	0.03432	0.13330	-1.39811E+01	1.67888E+01	-5.20889E+00
50	0.04290	0.13330	-1.38154E+01	2.62370E+01	1.29900E-02
51	0.05148	0.13330	-1.36031E+01	2.28750E+01	1.84167E-02
52	0.06006	0.13330	-1.34106E+01	2.19563E+01	1.84166E-02
53	0.06864	0.13330	-1.32229E+01	2.18018E+01	-1.86626E-02
54	0.07722	0.13330	-1.30385E+01	2.13848E+01	-1.86626E-02
55	0.08580	0.13330	-1.28544E+01	2.14625E+01	0.00000E+00
56	0.00000	0.16663	2.90819E+01	-8.20106E+03	6.69754E+01
57	0.00858	0.16663	-1.32432E+01	-5.29061E+02	-2.71480E+01
58	0.01716	0.16663	-1.41034E+01	-2.96251E+00	-1.66998E+00
59	0.02574	0.16663	-1.41135E+01	-4.42085E-01	-3.11330E-01
60	0.03432	0.16663	-1.39724E+01	1.74443E+01	6.71829E+00
61	0.04290	0.16663	-1.38113E+01	2.38325E+01	-4.96427E-01
62	0.05148	0.16663	-1.36069E+01	2.38325E+01	-4.96427E-01
63	0.06006	0.16663	-1.34106E+01	2.18018E+01	-1.86626E-02
64	0.06864	0.16663	-1.32235E+01	2.18018E+01	-1.86626E-02
65	0.07722	0.16663	-1.30386E+01	2.14625E+01	0.00000E+00
66	0.08580	0.16663	-1.28544E+01	2.14625E+01	0.00000E+00
67	0.00000	0.19996	3.04268E+01	-8.36422E+03	4.10107E+01
68	0.00858	0.19996	-1.30226E+01	-6.30326E+02	7.11257E+00
69	0.01716	0.19996	-1.40915E+01	-2.04539E+00	9.85857E-01

70	0.02574	0.19996	-1.41255E+01	1.68276E+01	5.25861E+00
71	0.03432	0.19996	-1.39811E+01	1.68276E+01	5.25861E+00
72	0.04290	0.19996	-1.38153E+01	2.62277E+01	-1.37740E-02
73	0.05148	0.19996	-1.36031E+01	2.28749E+01	-1.85242E-02
74	0.06006	0.19996	-1.34106E+01	2.19569E+01	-1.85242E-02
75	0.06864	0.19996	-1.32229E+01	2.18018E+01	1.87087E-02
76	0.07722	0.19996	-1.30385E+01	2.13846E+01	1.87087E-02
77	0.08580	0.19996	-1.28544E+01	2.14625E+01	0.00000E+00
78	0.00000	0.23328	3.17745E+01	-8.37652E+03	3.19841E+01
79	0.00858	0.23328	-1.30848E+01	-2.02673E+03	-1.69270E+02
80	0.01716	0.23328	-1.41006E+01	1.12604E+01	8.60107E-01
81	0.02574	0.23328	-1.41169E+01	-3.41704E+00	2.02267E-01
82	0.03432	0.23328	-1.39964E+01	1.54589E+01	-1.52158E+00
83	0.04290	0.23328	-1.38064E+01	2.29022E+01	5.82274E-01
84	0.05148	0.23328	-1.36036E+01	2.28484E+01	-1.37740E-02
85	0.06006	0.23328	-1.34111E+01	2.19569E+01	1.05765E-02
86	0.06864	0.23328	-1.32227E+01	2.19569E+01	1.05765E-02
87	0.07722	0.23328	-1.30379E+01	2.13846E+01	0.00000E+00
88	0.08580	0.23328	-1.28544E+01	2.13846E+01	0.00000E+00
89	0.00000	0.26661	3.30732E+01	-8.50807E+03	4.09423E+01
90	0.00858	0.26661	-1.31670E+01	-2.92030E+02	-6.59520E+01
91	0.01716	0.26661	-1.40958E+01	-2.57167E+00	-7.99016E-01
92	0.02574	0.26661	-1.41124E+01	1.04042E+01	2.25980E-01
93	0.03432	0.26661	-1.40100E+01	2.75647E+01	5.13087E-01
94	0.04290	0.26661	-1.38035E+01	2.67078E+01	-4.94524E-01
95	0.05148	0.26661	-1.36035E+01	2.29433E+01	-6.04121E-03
96	0.06006	0.26661	-1.34108E+01	2.19811E+01	4.78094E-03
97	0.06864	0.26661	-1.32223E+01	2.19569E+01	1.05765E-02
98	0.07722	0.26661	-1.30378E+01	2.13405E+01	1.05765E-02
99	0.08580	0.26661	-1.28544E+01	2.13846E+01	0.00000E+00
100	0.00000	0.29993	1.70141E+38	1.70141E+38	1.70141E+38
101	0.00858	0.29993	1.70141E+38	1.70141E+38	1.70141E+38
102	0.01716	0.29993	1.70141E+38	1.70141E+38	1.70141E+38
103	0.02574	0.29993	-2.52721E-01	-4.59297E+03	3.12038E+03
104	0.03432	0.29993	-1.40262E+01	4.98050E+01	5.56818E+00
105	0.04290	0.29993	-1.38007E+01	2.20174E+01	-5.35175E-02
106	0.05148	0.29993	-1.36071E+01	2.36481E+01	-1.91827E-02
107	0.06006	0.29993	-1.34112E+01	2.19110E+01	-1.91827E-02
108	0.06864	0.29993	-1.32227E+01	2.19811E+01	-8.82150E-02
109	0.07722	0.29993	-1.30376E+01	2.14380E+01	-8.82150E-02
110	0.08580	0.29993	-1.28544E+01	2.13405E+01	0.00000E+00

111	0.00000	0.33326	1.70141E+38	1.70141E+38	1.70141E+38
112	0.00858	0.33326	1.70141E+38	1.70141E+38	1.70141E+38
113	0.01716	0.33326	1.70141E+38	1.70141E+38	1.70141E+38
114	0.02574	0.33326	1.70141E+38	1.70141E+38	1.70141E+38
115	0.03432	0.33326	-1.29702E+01	-3.29089E+02	2.21887E+02
116	0.04290	0.33326	-1.37952E+01	2.27185E+01	-4.02840E-02
117	0.05148	0.33326	-1.36003E+01	2.27185E+01	-4.02840E-02
118	0.06006	0.33326	-1.34077E+01	2.21324E+01	1.30200E-01
119	0.06864	0.33326	-1.32178E+01	2.21324E+01	1.30200E-01
120	0.07722	0.33326	-1.30349E+01	2.10306E+01	2.85185E-01
121	0.08580	0.33326	-1.28544E+01	2.10306E+01	2.85185E-01

ENTER 0 FOR CURRENT AND NEXTPOINT

1 FOR 2D PRINTING

2 FOR 2D PLOTTING

3 FOR CURRENT AND STOPPING

4 FOR CHANNEL PRINTING

3 (user input)

Vg = 3.000 Vd = 0.250 Vfb = -0.560 Q = 0.0000E+00 current 5.3089E-05

# FEDERAL INFORMATION PROCESSING STANDARD SOFTWARE SUMMARY

01. Summary date			02. Summary prepared by (Name and Phone)			03. Summary action		
Yr.	Mo.	Day	C. L. Wilson (301) 921-3541			New	Replacement	Deletion
8	4	03	05. Software title			<input checked="" type="checkbox"/>	<input type="checkbox"/>	<input type="checkbox"/>
04. Software date			CSLR: A Two-Dimensional Finite Element Charge-Sheet			Previous Internal Software ID		
Yr.	Mo.	Day	Model of MOSFETs Including Radiation-Induced Inter-					
8	4	03	face and Oxide Charge					
06. Short title						07. Internal Software ID		

08. Software type	09. Processing mode	10. Application area	
		General	Specific
<input type="checkbox"/> Automated Data System <input checked="" type="checkbox"/> Computer Program <input type="checkbox"/> Subroutine/Module	<input checked="" type="checkbox"/> Interactive <input checked="" type="checkbox"/> Batch <input type="checkbox"/> Combination	<input type="checkbox"/> Computer Systems Support/Utility <input checked="" type="checkbox"/> Scientific/Engineering <input type="checkbox"/> Bibliographic/Textual	<input type="checkbox"/> Management/Business <input type="checkbox"/> Process Control <input type="checkbox"/> Other

11. Submitting organization and address National Bureau of Standards Washington, DC 20234	12. Technical contact(s) and phone C. L. Wilson 921-3541 J. L. Blue 921-3395
---	--

13. Narrative

A two-dimensional charge-sheet model including radiation-induced interface and oxide effects in short-channel MOS transistors has been developed. The primary effect of ionizing radiation on MOSFETs is the introduction of oxide trapped charge (OTC), interface trapped charge (ITC), and the reduction of channel mobility caused by scattering from charge in interface traps.

14. Keywords

Finite elements; MOS transistor; radiation effects

15. Computer manuf'r and model VAX	16. Computer operating system VMS	17. Programing language(s) FORTRAN	18. Number of source program statements
19. Computer memory requirements 200K	20. Tape drives 0	21. Disk/Drum units 0	22. Terminals 1

23. Other operational requirements

Requires local interactive vector-oriented graphics

24. Software availability	25. Documentation availability
Available <input type="checkbox"/> Limited <input checked="" type="checkbox"/> In-house only <input type="checkbox"/> C. L. Wilson 925-3541 9-track 1600bpi ASCII magnetic tape, DNA approved users only	Available <input checked="" type="checkbox"/> Inadequate <input type="checkbox"/> In-house only <input type="checkbox"/> Title as in section 05.

26. FOR SUBMITTING ORGANIZATION USE

U.S. DEPT. OF COMM. <b>BIBLIOGRAPHIC DATA SHEET</b> <i>(See instructions)</i>	<b>1. PUBLICATION OR REPORT NO.</b> NBSIR 84-2874R	<b>2. Performing Organ. Report No.</b>	<b>3. Publication Date</b> May 1984
<b>4. TITLE AND SUBTITLE</b> CSLR: A Two-Dimensional Finite Element Charge-Sheet Model of MOSFETs Including Radiation-Induced Interface and Oxide Charge			
<b>5. AUTHOR(S)</b> C. L. Wilson and J. L. Blue			
<b>6. PERFORMING ORGANIZATION</b> <i>(If joint or other than NBS, see instructions)</i> <b>NATIONAL BUREAU OF STANDARDS</b> <b>DEPARTMENT OF COMMERCE</b> <b>WASHINGTON, D.C. 20234</b>		<b>7. Contract/Grant No. Task No.</b> X99QAXVX, Work Unit 00076	<b>8. Type of Report &amp; Period Covered</b>
<b>9. SPONSORING ORGANIZATION NAME AND COMPLETE ADDRESS</b> <i>(Street, City, State, ZIP)</i> Defense Nuclear Agency Washington, DC			
<b>10. SUPPLEMENTARY NOTES</b> <input checked="" type="checkbox"/> Document describes a computer program; SF-185, FIPS Software Summary, is attached.			
<b>11. ABSTRACT</b> <i>(A 200-word or less factual summary of most significant information. If document includes a significant bibliography or literature survey, mention it here)</i> A two-dimensional charge-sheet model including radiation-induced interface and oxide effects in short-channel MOS transistors has been developed. The unique feature of the model is that the effects of channel inversion layer charge, interface charge, and oxide charge are included as a nonlinear integral boundary condition on the two-dimensional electrostatic field in the transistor. The average inversion layer charge density and source-drain current are obtained directly from the model rather than from the electron density or electron quasi-Fermi level. The model retains all of the physical detail of more complex two-dimensional models such as sensitivity to source-drain profile shape, channel profile, and oxide field shape. This allows the model to represent the changes in drain current associated with short-channel effects while still allowing simple comparison with long-channel models. The numerical solutions were obtained using general-purpose software for solving elliptic partial differential equations. Problems with exact solutions have been solved <del>to test the correctness and accuracy of the codes. Also, the physics included in this model and the geometry of the transistor can be easily changed.</del> The finite element method used allows refinement of oblique triangles which is important in achieving computational efficiency.			
<b>12. KEY WORDS</b> <i>(Six to twelve entries; alphabetical order; capitalize only proper names; and separate key words by semicolons)</i> Finite elements; interactive graphics; MOS transistors; radiation effects.			
<b>13. AVAILABILITY</b> <input type="checkbox"/> Unlimited <input checked="" type="checkbox"/> For Official Distribution. Do Not Release to NTIS <input type="checkbox"/> Order From Superintendent of Documents, U.S. Government Printing Office, Washington, D.C. 20402. <input type="checkbox"/> Order From National Technical Information Service (NTIS), Springfield, VA. 22161		<b>14. NO. OF PRINTED PAGES</b> 50	<b>15. Price</b>



